Title

Rapid Detection of Disease Biomarkers Using Novel Hydrogel Beads

Author

Zhang, Hanxu

Publication Date

2022

Peer reviewed|Thesis/dissertation

UNIVERSITY OF CALIFRONIA

Los Angeles

Rapid Detection of Disease Biomarkers Using Novel Hydrogel Beads

A thesis submitted in partial satisfaction

of the requirements for the degree Master of Science

in Bioengineering

by

Hanxu Zhang

2022

ABSTRACT OF THE THESIS

Rapid Detection of Disease Biomarkers Using Novel Hydrogel Beads

by

Hanxu Zhang

Master of Science in Bioengineering

University of California, Los Angeles, 2022

Professor Daniel T. Kamei, Chair

Hydrogels are multifunctional biomaterials popularly used in a wide range of applications. In this thesis, calcium alginate hydrogels were thoroughly studied with a special focus on synthesizing calcium alginate hydrogel beads using a simple set up involving only a syringe and a gelation bath. By introducing an additional nonionic polymer component to the alginate solution during synthesis, the hydrogel beads exhibited greatly improved morphology with regard to uniformity and sphericity. These hydrogel beads also demonstrated excellent dye retention properties and stability in water. Additionally, they exhibited a gel-sol transition process in response to external stimuli such as calcium chelators.

Taking advantage of these properties, the novel hydrogel beads were integrated in diagnostics applications for point-of-care detection of metabolic alkalosis and biomarkers in bacterial infections, with the degradation of gel and release of dye as disease indicators. For metabolic alkalosis detection, the assay utilized the reaction of sodium bicarbonate and citric acid to produce citrate, a metal chelator capable of competitively binding to calcium cations in the gel

matrix to trigger hydrogel degradation. This resulted in successful detection of elevated bicarbonate concentrations in less than one hour. For detection of biomarkers in bacterial infections, novel hydrogel beads were synthesized with an additional enzyme substrate component in their gel matrix, which allowed for substrate cleavage and gel degradation to occur in the presence of bacterial enzymes. Results from preliminary studies showed that the gel-sol response of the hydrogel beads towards the bacterial enzymes α-amylase and trypsin was successfully achieved.

The thesis of Hanxu Zhang is approved.

Benjamin M. Wu

Jun Chen

Daniel T. Kamei, Committee Chair

University of California, Los Angeles

2022

TABLE OF CONTENTS

TABLE OF FIGURES

ACKNOWLEDGMENTS

The completion of this thesis would not have been achieved without the endless support from my mentor, friends, and family.

My biggest thanks go out to my mentor Dr. Daniel T. Kamei. I joined the Kamei lab initially because of my interest in diagnostics, but what made me truly stay and look forward to going to lab everyday was its warm family culture that Dr. Kamei and everyone in the lab created. Dr. Kamei is the best mentor that any researcher can ask for - he went out of his way to teach and support me every step of the way from when I joined the lab in March 2020 to my master's graduation in June 2022. Because of his constant support, encouragement, and advice, I grew substantially as both a researcher and a person. I would especially like to thank him for pushing me in the kinetics modeling subgroup. It was undoubtedly the most challenging time in my lab experience, but it made me truly understand what it takes to be a good bioengineer and researcher.

My next thanks go to Paula Pandolfi, who I got to work very closely with throughout the past year. I am very grateful to have her as my partner in the hydrogel subgroup for everything she's contributed to our project. Without her passion and dedication to research, this project would not have been where it is at right now. I would also like to thank Paula for being the most amazing friend - her positive energies and willingness to help others brought everyone in lab closer. I will miss running trials with her, all our hangouts, and all the conversations that we had.

I would like to thank Yui Nadalin, who I also worked closely with in the past year. Yui is an amazing undergraduate researcher to have on our team, not only did she give her a hundred

percent when running trials in lab, she would also constantly come up with insightful ideas to help push our project forward. Her presence would always bring light to the lab.

The past year in lab also would not have been the same without all the rest of the "overgrads", Jerry Lu, Frances Nicklen, Alexia Diaz, Jasmine Trinh, Milo Ryan, and Salil Patel. They are a group of hard-working, self-driven, humorous, and kind people and they inspire me everyday. The banters that we share in the office will be dearly missed.

Lastly, I would like to thank my family for their support and love. My parents first inspired my interest in diagnostics, and their endless support, invaluable advice, and unconditional love helped shape me into the person I am today. My grandparents' unconditional love and care also continued to motivate and inspire me even though they are thousands of miles away.

Chapter 2 is a version of P. Pandolfi, H. Zhang, Y. Nadalin, M. Prasetyo, A. Toubian, B.M. Wu, and D.T. Kamei. *Degradation of Hydrogel Beads for the Detection of Serum Bicarbonate Levels for the Diagnosis of Metabolic Alkalosis at the Point of Care*, which is in preparation for submission. D. T. Kamei was the director of research for this article. This project was supported by UCLA funds.

Chapter 1. Motivation and Background

1.1 Hydrogels

Hydrogels are systems of three-dimensional crosslinked networks. They are hydrophilic and thus have the capability of absorbing and retaining large quantities of water, resulting in the swelling of their solid gel matrix. Hydrogels are advantageous in many ways. First, due to their soft and flexible gel nature, their sizes and shapes are easily tunable. They are often responsive towards external stimuli such as temperature, pH, light, and chemicals.[1] In addition, as most hydrogels are made of naturally derived materials such as polypeptides or polysaccharides, they are highly biocompatible and biodegradable. These advantages make hydrogels popular candidates for use in a wide range of bioengineering applications such as tissue engineering,[2] cell encapsulation,[3,4,5] biofabrication,[6,7] drug delivery,[8] therapeutics,[9] biosensing,[10] and diagnostics.[11]

There are a wide variety of materials employed to synthesize hydrogels such as polysaccharides and proteins. For example, the most common polysaccharides used for generating hydrogels are agarose, alginate, chitosan, cellulose, and hyaluronic acid,[12] while the most commonly used proteins are collagen and gelatin.[12] Multiple materials have been extensively studied in their ability to form copolymers that can form hydrogels. One such example is the crosslinking between collagen and glycosaminoglycans (GAGs) to form hydrogels with unique properties.[13]

There are two main categories of hydrogel synthesis methods: physical crosslinking and chemical crosslinking. Chemically crosslinked hydrogels are formed by covalent bonds between molecules.[14] Processes to achieve this include polymer-polymer conjugation, enzymatic crosslinking, and crosslinking polymer chains with the addition of crosslinker molecules or photosensitive agents.[15] Chemically crosslinked hydrogels are highly versatile with easily tunable

gel properties.[16] They also generally have strong mechanical properties, great stability, and long durability due to the strong interactions associated with covalent bonds.[17] However, chemical crosslinking often requires toxic compounds which need to be removed before a synthesized gel can be used for biological applications. Moreover, the use of crosslinking agents can also generate unwanted biproducts inside the gel matrix,[16] impeding the biocompatibility of the gels. On the other hand, physical crosslinked hydrogels avoid such adverse effects and have much easier synthesis procedures. They are formed by noncovalent bonds, i.e., weak interactions, between polymer chains without the need for organic solvents or toxic chemical crosslinking agents.[16] Processes that achieve physical crosslinking include hydrophobic interactions, hydrogen bonding, crystalline formation, and ionic crosslinking.[15] One notable property of crosslinked gels is that they can typically undergo reversible sol-gel transitions in certain conditions due to their relatively weak bonds.[18]

Ionic crosslinking is one of the simplest and mildest processes used to synthesize physically crosslinked hydrogels.[19] It occurs when oppositely charged species crosslink through attractive electrostatic interactions. More specifically, this process usually occurs between a charged polymer (polyelectrolyte) and an ion, or between two polyelectrolytes. Besides having the advantage of being biocompatible, the links between ionic crosslinked hydrogels are also non-permanent and reversible, making them multifunctional in many applications. Some common examples of hydrogels that are synthesized with this method include the ionic crosslinking between acrylic polymers containing copolymerizable acid groups with multivalent metal ions such as zinc and chromium.[20] Another example is the ionic complexing between the polycation chitosan with polyanions such as polyacrylic acid, polyphosphoric acid, pectin, and alginate.[20] Natural

polysaccharide alginate can also undergo ionic crosslinking with divalent metal cations such as Ca^{2+}, Mg^{2+}, and Fe^{2+}.[20]

1.2 Alginate Hydrogels

Alginate is one of the most commonly used biomaterials for ionic crosslinked hydrogels. Alginate is a naturally occurring complex carbohydrate derived from marine brown algae and some bacteria.[21] The polysaccharide is comprised of sugars β-d-mannuronic and α-l-guluronic acid linked in various compositions and sequences via their 1,4-glycosidic bonds. Its chemical molecular structure is shown in Figure 1-1.

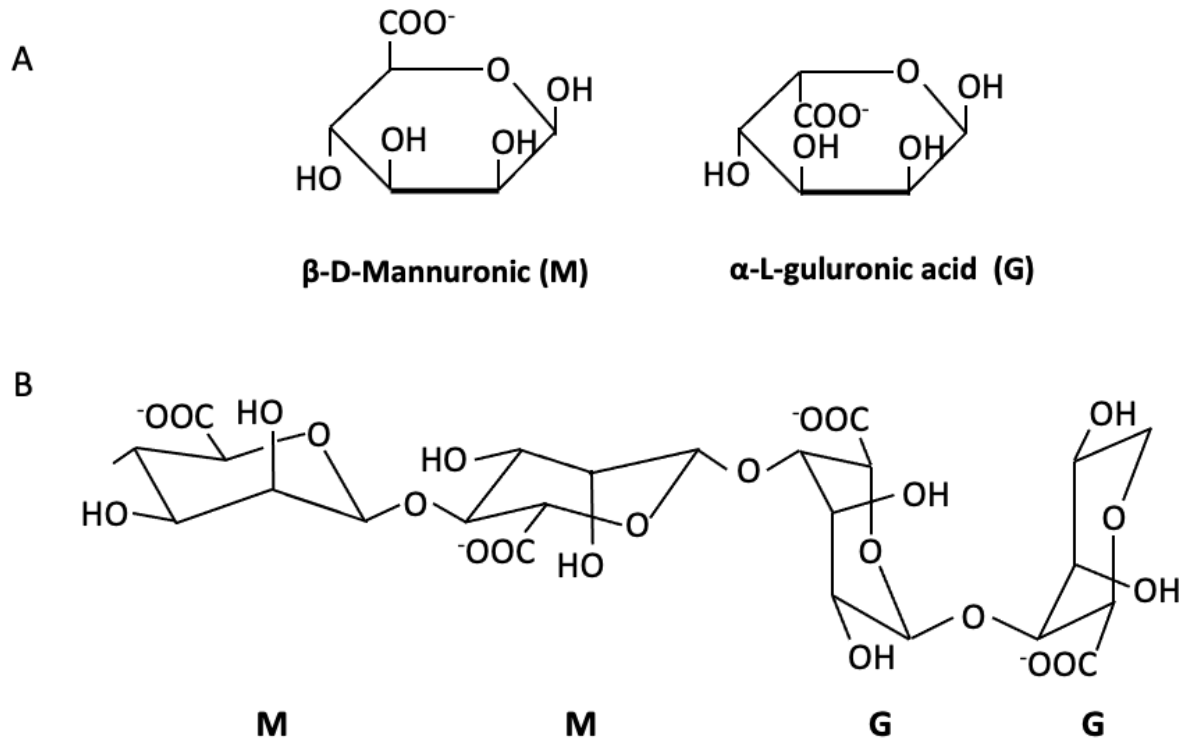

Figure 1-1. Structures of alginate

The polysaccharides are soluble in water. When divalent cations such as Ca^{2+}, Mg^{2+}, and Fe^{2+} are present, alginate undergoes a sol-gel transition to form a gel matrix via ionic crosslinking

with the cations. Specifically, metal cations bind to the negatively charged alginate polymers[22] to form a three-dimensional woven network of polymers. There have been various models developed to describe the structure of metal alginate hydrogels, of which, the egg-box model is the most commonly accepted description (Figure 1-2).[23] The model proposes that 10 oxygen atoms from each acid block coordinate a single metal ion thereby resulting in a egg-box-like gel structure.[23]

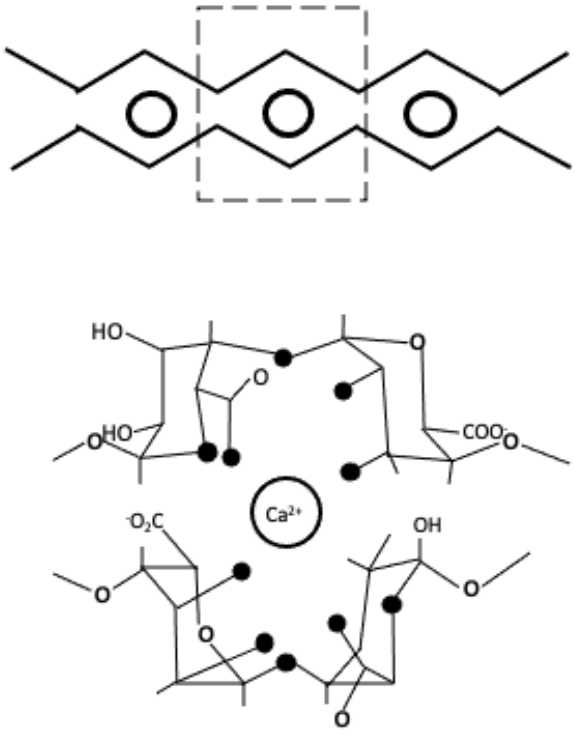

Figure 1-2. Egg-box model of calcium alginate

There are many advantages to using alginate gels in various applications such as wound healing, drug delivery, and tissue engineering.[21] Alginate is biocompatible, biodegradable, and low in cost. It also has a high stability and can encapsulate biomolecules and cells. In addition, their mechanical strength and porosity are adjustable.[21] Another notable trait of alginate hydrogels is

the reversible sol-gel transition in response to certain metal chelators as well as specific cleaving enzymes such as alginate lyase.[24,25,26]

Alginate gels are commonly synthesized using methods such as the internal setting method and the diffusion method. The internal setting method involves slow gelation mediated by a change in pH which releases metal ions from an insoluble salt slowly to crosslink with the alginate polymers.[27] The diffusion method is a simpler and faster process. The most basic form of the diffusion method is also called the extrusion dripping method, where an alginate solution is extruded into a gelation bath containing divalent metal ions.[28] However, the crosslinked alginate gel synthesized by this method usually has low mechanical strength and low uniformity.[29] This is because the direct mixing of alginate and divalent cations can easily result in the inhomogeneity of the gel due to the strong and fast crosslinking mechanism.[21] In our work, a simple and rapid alginate gel bead synthesis strategy was developed to improve the uniformity of the alginate gels.

1.3 Integration of Alginate Hydrogels in Point-of-Care Diagnostics

Point-of-care testing corresponds to diagnostics performed outside a laboratory setting and at the site of patient care or at home. The World Health Organization stipulated a set of criteria, termed the ASSURED criteria, to describe point-of-care diagnostics.[30] These criteria indicate that point-of-care diagnostics should be affordable, sensitive, specific, user-friendly, rapid and robust, equipment-free, and deliverable. Point-of-care diagnostics are usually developed for resource-limited settings, but they can also provide many benefits in hospital settings such as in the emergency department, as they can help enable more rapid decision-making processes for clinicians in choosing treatments and diagnosing diseases and conditions. In addition, they can also help avoid problems with patient sample transport. With rising incidences of infectious

diseases such as SARS-CoV-2, HIV, and influenza, there is also a growing need for point-of-care diagnostics to mitigate disease progression globally.[31]

Hydrogels have recently gained more popularity for use in the development of diagnostic assays. Within the class of hydrogels, alginate hydrogels have garnered much attention. An alginate hydrogel scaffold incorporating TiO2 nanotubes was developed to rapidly sense lactate and glucose in sweat.[32] An immunosensor for a tumor marker was also developed using calcium-triggered precipitation of sodium alginate.[33] Moreover, a sensing interface for an electrochemical immunosensor was developed with the incorporation of iron alginate hydrogels.[34] Microneedle arrays coated with calcium alginate hydrogels were also developed for sampling and sensing nucleic acids in interstitial fluid from the skin.[35] However, most of these detection assays are not suitable for point-of-care settings, and all of them require complex synthesis procedures that prevent their production in resource-limited settings. In this thesis, we developed a point-of-care diagnostic assay via a simple synthesis of a novel alginate gel system.

1.4 Concluding Remarks and Thesis Overview

In this thesis, we studied calcium alginate hydrogels thoroughly with a special focus on synthesizing calcium alginate hydrogel beads using a set up that is much simpler and more low-cost than conventional synthesis procedures. Specifically, novel spherical hydrogel beads with uniform radii were synthesized by manually dispensing a solution using only a syringe into a gelation bath. This simple process eliminated complex steps and equipment (such as a syringe pump, a stir plate, and hot plate) typically seen in conventional synthesis procedures like the extrusion dripping method.[28] To develop our simple processing method, we incorporated an additional nonionic polymer component to the alginate solution when synthesizing hydrogel beads,

which resulted in hydrogel beads with greatly improved morphology with regard to uniformity and sphericity in comparison to calcium alginate hydrogel beads at the low calcium alginate concentrations of interest in our applications. These hydrogel beads also demonstrated excellent dye retention properties and stability in water. Additionally, they exhibited a gel-sol transition process in response to external stimuli such as calcium chelators, which allowed their use in visually detecting disease biomarkers.

Inspired by past work performed by other groups on the development of hydrogel diagnostic assays, we focused on developing novel hydrogel beads that could be synthesized and used in resource-taxed areas. Chapter 2 describes the development of a point-of-care diagnostic assay for metabolic alkalosis. It is a version of P. Pandolfi, H. Zhang, Y. Nadalin, M. Prasetyo, A. Toubian, B.M. Wu, and D.T. Kamei. *Degradation of Hydrogel Beads for the Detection of Serum Bicarbonate Levels for the Diagnosis of Metabolic Alkalosis at the Point of Care*, which is in preparation for submission. Chapter 3 summarizes our preliminary investigation of using the novel hydrogel beads for the detection of bacteria.

Chapter 2. Point-of-Care Detection of Metabolic Alkalosis

2.1 Introduction

A hydrogel is a three-dimensional network of polymer chains immersed in a water-rich environment that possesses a myriad of physicochemical properties which allow for versatile applications in many areas of research.[36] In bioengineering, current research explores the application of hydrogels to tissue regeneration,[2] cell encapsulation,[4,5,19] biofabrication,[7] drug delivery,[8] biosensing,[10] and diagnostics.[11] Notable examples of hydrogel diagnostic applications include incorporation of hydrogels with lateral-flow immunoassays for the detection of SARS-CoV-2,[11] multifunctional colorimetric monitoring of pH and glucose levels in chronic wounds in diabetic patients,[37] and hydrogel-based microfluidic assays for the rapid detection of biomarkers that delay wound healing.[38] Another example is the application of hydrogels for bacterial detection through chemical modification of the hydrogel components with colorimetric substrates. Enzymes specific to different bacteria strains catalyzed cleavage reactions that induced the release of colorimetric markers for visual detection of the specific strains by the naked eye.[10] However, all of these methods introduced many complexities to the synthesis of the hydrogel system due to the need for chemically modifying the hydrogel components in order to create a matrix with specificity towards the biomarker of interest.[10,11,37,38] Inspired by the application of hydrogels that produce simple, easy to read colorimetric results, we designed a diagnostic with easily interpretable results that uses hydrogels that require minimal labor, inexpensive reagents, and equipment to synthesize.

A commonly used hydrogel-forming polymer is alginate, which exhibits low toxicity, high biocompatibility, low cost, and innate gelation properties.[39] Alginate is a naturally occurring polysaccharide co-polymer that is composed of 1,4-linked β-d-mannuronic acid and α-l-glucuronic acid blocks in varying compositions and sequences.[39] One notable property of alginate is its ability

to bind to divalent cations through the process of ionic crosslinking in order to form hydrogels.[40] Ionic crosslinking is a spontaneous process that occurs due to electrostatic attractive interactions between positively charged divalent cations such as calcium and negatively charged carboxyl functional groups in the alginate polymer chains. This interaction between calcium and alginate results in an intricately woven network of the alginate polymers that form a calcium alginate gel.[40] Notably, this reaction is reversible as the calcium alginate gel network can be disassembled in response to various external stimuli such as the introduction of a metal chelator, which can be advantageous in many applications.[41] The disassembling of the gel network could cause the release of encapsulated dye molecules, resulting in a more robust visual output that can be easily interpreted by untrained personnel at the point of care (POC). Thus, calcium alginate gels have the potential for use in POC settings like mobile clinics due to their ease of synthesis, versatility, low cost, ability to retain dye for visual colorimetric detection, and their sensitivity towards external stimuli.

Our research focuses on the development of a POC device for the detection of metabolic alkalosis. Metabolic alkalosis results from the disruption of the acid-base equilibrium in the body and is commonly related to kidney disease, hyperparathyroidism, and excess vitamin D levels. In metabolic alkalosis, there is either a net accumulation of base or a loss of acid in the blood often caused by chloride ion depletion from excessive vomiting, diuretic abuse, starvation, or chloride deficient diets, many of which are common in hospital patients. Consequently, a surplus of bicarbonate ions are present in the body which can lead to an elevated physiological pH, compromising cell and organ functions.[42] Normal serum levels of bicarbonate range from a concentration of 22 to 29 mmol/L. Samples with serum bicarbonate concentrations of 30-40 mmol/L are indicative of alkalosis, yet most patients fail to present immediate symptoms. In severe

alkalosis cases, serum bicarbonate concentrations can range from 40 to 50 mmol/L, causing patients to experience various levels of hypoxemia. Above 50 mmol/L, the patient is at great risk for seizures, altered mental states, and coma.[43] Severe cases of metabolic alkalosis that present significantly elevated blood pH have 45-80% mortality rates, highlighting the importance of early disease detection.[44] Current gold standard diagnostics rely on a combination of an electrolyte panel and arterial blood gas analysis, requiring a long time-to-result, expensive lab equipment, significant power, and trained personnel. Thus, there is a need to develop a rapid and efficient diagnostic to detect bicarbonate levels for early stage metabolic alkalosis so that blood pH can be restored to safe levels in a timely manner. This work introduces such a device through utilizing the physicochemical degradation properties of calcium alginate dextran (CaAD) hydrogel beads for the detection of metabolic alkalosis at the POC.

Our detection assay takes advantage of the reaction between bicarbonate and citric acid to form citrate, a strong metal chelator. The resultant reaction between citrate and calcium in the hydrogel will result in the degradation of the hydrogel beads, allowing for simple disease detection by the naked eye. Degradation rates of the hydrogel beads could therefore be directly correlated with bicarbonate concentration. However, conventional calcium alginate beads made with simple procedures would take a long time to degrade at even elevated levels of serum bicarbonate due to the high levels of calcium that would need to be chelated away from the hydrogel. In order to increase the rate of degradation and allow for a rapid time to result, the calcium alginate concentration in the beads was decreased, but this negatively affected the spherical morphology of the beads, resulting in misshapen beads and inconsistent degradation rates. We therefore hypothesized that the addition of a nonionic polymer, such as dextran, would aid in the formation of the spherical hydrogel beads without increasing time to result due to being uncharged and

therefore unable to participate in the ionic crosslinking. With the introduction of the nonionic polymer dextran, we were able to reduce the calcium alginate concentration and still synthesize homogeneous spherical beads with a very simple procedure that degraded at elevated bicarbonate levels in the short times necessary for use at the POC.

2.2 Materials and Methods

2.2.1 Preparation of the polymer solution and gelation bath

All reagents and materials were purchased from Sigma-Aldrich (St. Louis, MO) unless otherwise noted. To synthesize calcium alginate hydrogel beads, a 1% w/w sodium alginate solution was first prepared in deionized water. Additionally, 0.25 mg of Coomassie Brilliant Blue G-250 dye (Fisher Scientific, Hampton, NH) in deionized water was added per 1 mL of polymer solution for hydrogel visualization. To observe the effects of different nonionic polymers on the ionic crosslinking mechanism and the overall hydrogel properties, polymer solutions were also prepared with 1% w/w sodium alginate and 20% w/w additional polymer in deionized water. The additional polymers tested had various molecular weights of dextran, polyethylene glycol (PEG), and ethylene oxide-*ran*-propylene oxide (EOPO). For the salt gelation bath, a 1% w/w calcium chloride solution was prepared in deionized water. To study bead morphology and dye retention properties at lower calcium alginate percentages, 0.4, 0.6, and 0.8% w/w sodium alginate solutions with either 20, 30, 40, or 50% w/w dextran 6k were prepared. For these trials, the gelation baths were made with 0.4, 0.6, and 0.8% w/w calcium chloride in deionized water, respectively.

2.2.2 Hydrogel synthesis

The simple experimental setup we employed for synthesizing the hydrogel beads is shown in Figure 2-1. A 1 mL Luer lock syringe (VWR, Radnor, PA) containing the polymer solution was positioned vertically with its attached 30G needle tip (Thomas Scientific, Swedesboro, NJ) and suspended approximately 10 cm above a glass scintillation vial (Fisher Scientific, Hampton, NH) containing the gelation bath. The syringe needed to be a certain height above the scintillation vial to ensure polymer droplets hit the gelation bath at a speed fast enough to allow for full immersion in the bath. This was to ensure uniform crosslinking during hydrogel formation to generate beads of the desired spherical geometry. The syringe plunger was gently pressed to continuously dispense polymer droplets. There was no stirring involved in the processing of beads. After the polymer solution was fully dispensed, the hydrogel beads were left to incubate in the gelation bath at room temperature for at least 1 h to allow for completion of the crosslinking reaction, further stabilizing the hydrogel matrix. After the incubation period, the hydrogel beads were collected and washed with deionized water to remove excess calcium chloride ions. To examine the morphology and dye release properties of different hydrogel beads, 20 beads of each type were stored in 3 mL of deionized water in a scintillation vial. Pictures were taken in a controlled lighting environment with an iPhone 12 camera (Apple, Cupertino, CA) immediately after placement in water, as well as after 8 days of incubation.

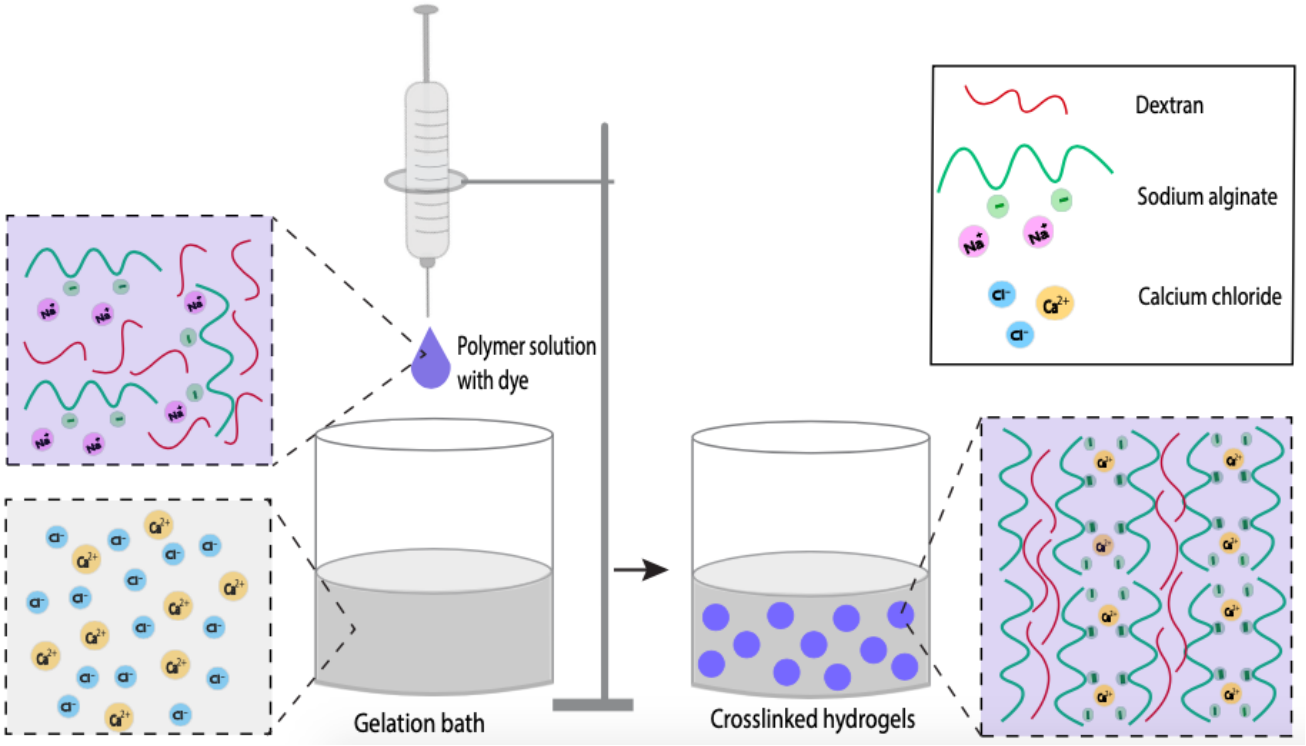

Figure 2-1. Schematic of the ionic crosslinking set up for CaAD hydrogel bead synthesis. Briefly, a polymer solution containing sodium alginate and dextran is dispensed dropwise into a gelation bath containing calcium chloride, allowing for the complexation between alginate polymers and calcium ions to form a spherical gel matrix instantaneously.

2.2.3 Degradation properties of hydrogel beads

Degradation rates of CaAD hydrogel beads in the presence of bicarbonate, citric acid, and citrate were studied separately. Ten beads made with 1% calcium alginate and 20% dextran 6k were incubated in 2 mL microcentrifuge tubes (VWR, Radnor, PA) containing either 1.5 mL of 50 mmol/L sodium bicarbonate in phosphate-buffered saline (PBS) (Gibco, Waltham, MA), 1.5 mL of 50 mmol/L citric acid in PBS, or 1.5 mL of 50 mmol/L sodium citrate in PBS. Additionally, 10 beads were incubated in PBS without sodium bicarbonate as a negative control. All tubes were placed on a nutator mixer (Clay Adams, New York, NY) at 12 RPM at room temperature. Pictures

were taken with an iPhone 12 camera when the degradation reaction was initiated (t=0 min), and each time complete degradation of hydrogel beads was observed.

2.2.4 Detection of bicarbonate

The detection of bicarbonate concentrations was carried out as follows for all hydrogel bead formulations and sample environments. Eight 2 mL microcentrifuge tubes were prepared with 1.485 mL of PBS or human serum (lot # 502036415, Fisher Scientific, Hampton, NH) spiked with varying concentrations of sodium bicarbonate (0, 20, 25, 30, 35, 40, 45, and 50 mmol/L). Next, 15 μL of citric acid in PBS at a concentration of 1 g/mL was added into each tube. 10 hydrogel beads were then transferred into each tube to start the degradation reaction. The tubes were placed on a nutator at 12 RPM at room temperature. Pictures of all tubes were taken with an iPhone 12 camera immediately after the degradation reaction started (t=0 min) and each time complete hydrogel bead degradation was observed.

2.2.5 Development of the point-of-care device

All parts were designed in Autodesk Fusion 360 and sliced in Ultimaker Cura. Parts were printed using the 3D printer Ultimaker 3 (Ultimaker, Utrecht, Netherlands). Structural components were printed using copolyester filament and joints were printed using thermoplastic polyurethane. The device was designed to house a DC 6V 10 RPM motor (Walfront, Lewes, DE) powered by a battery pack containing 4 AA batteries connected in a simple circuit. Due to the applied load, the resulting rotational speed of the motor was estimated to be 9 RPM. The motor was used to rotate a 2 mL microcentrifuge tube and its housing about its horizontal axis. The rotational speed of the

device was further adjusted with the use of a 2:1 gear system to increase the RPM to a desired value of approximately 18.

2.3 Results and Discussion

2.3.1 Hydrogel bead morphology studies

As shown in Figure 2-2A, 1% calcium alginate hydrogel beads synthesized without an additional nonionic polymer were neither spherical nor uniform in size. In order to develop a robust diagnostics assay that depended on bead degradation rates, it was essential to find a hydrogel bead formulation that consistently yielded uniform and spherical beads at low calcium alginate concentrations. For this reason, we introduced a nonionic polymer to the alginate solution when synthesizing the hydrogel beads. Interestingly, all of the hydrogel beads synthesized with 1% calcium alginate and 20% nonionic polymer showed better morphologies overall, demonstrated by their spherical shapes. More specifically, PEG 4.6k, PEG 20k, and dextran 6k beads showed the best morphologies in terms of monodispersity and spherical geometry. On the other hand, while EOPO and dextran 35-45k beads were uniform and appeared spherical from the top view (Figure 2A), they were flatter and appeared disk-like when observed from the side view (Figure 2B). This was unfavorable because disc-shaped beads are more difficult to visualize from the side, hindering the visual detection of degradation. It is currently unclear why the addition of a second polymer improves bead morphology. Presumably, a nonionic polymer can add bulk to the hydrogel beads without increasing rates of degradation since it is uncharged. In addition, the change in viscosity and/or surface tension of the polymer solution could also be factors, but further studies are necessary to confirm these possible reasons.

2.3.2 Stability and dye retention

To develop a diagnostic assay with a long shelf-life, it is necessary for the hydrogel beads to be both stable in water and capable of retaining dye for an extended period of time. Therefore, the stability and dye release properties of the hydrogel beads were studied over time. As shown in Figure 2-2B, all hydrogel beads retained their original morphologies in deionized water over 8 days, indicating good stability. The dye release experiments demonstrated that hydrogel beads containing the nonionic polymer dextran 6k had the best dye retention. For all other hydrogel beads, there was an increase of dye in water visible to the naked eye after 8 days. More specifically, PEG 4.6k and dextran 35-45k beads exhibited slight release, followed by greater release from EOPO 12k beads and the most release from PEG 20k beads. As a result, dextran 6k was selected as the nonionic polymer to be added to the alginate solution for hydrogel bead synthesis.

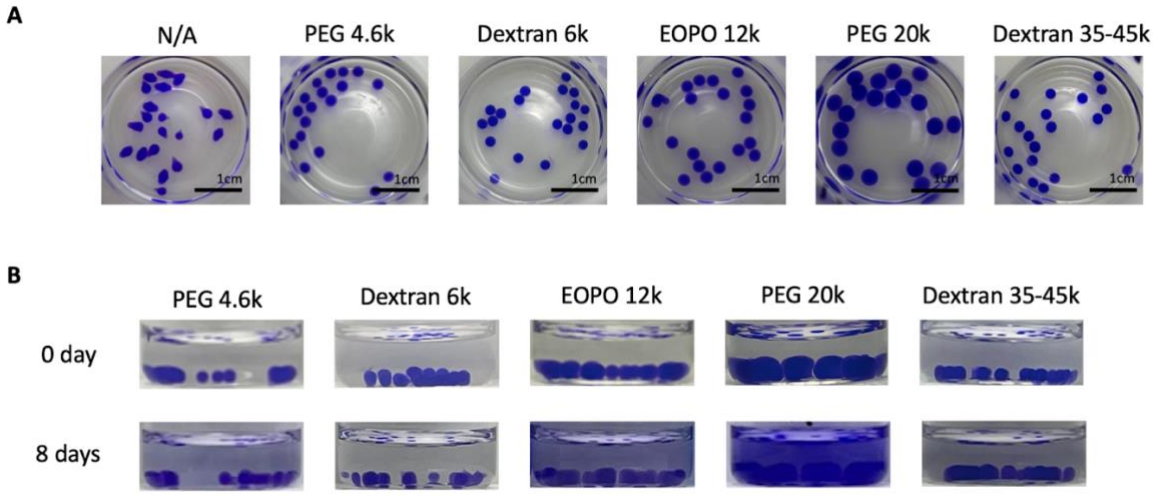

Figure 2-2. Morphology and release behavior of 1% calcium alginate hydrogel beads synthesized with and without an additional nonionic polymer in the polymer solution. (A) Overall morphology of the different hydrogel compositions. The leftmost hydrogel beads contained no additional polymer, while the others (from left to right) contained 20% PEG 4.6k, 20% dextran 6k, 20% EOPO 12k, 20% PEG 20k, and 20% dextran 35-45k. (B) Dye release study. From left to right, the beads were made with 20% PEG 4.6k, 20% dextran 6k, 20% EOPO 12k, 20% PEG 20k, and 20% dextran 35-45k.

2.3.3 Dextran hydrogel bead degradation studies

While the hydrogel beads were shown to have good stability in water, calcium alginate gels are also known to be responsive to various external stimuli. One such example is the gel-sol transition response of the calcium alginate gel in the presence of certain metal chelators as well as enzymes such as alginate ligase.[45,26] In our assay, the degradation properties of the hydrogels assisted by calcium chelators were utilized to achieve the visual detection of high levels of bicarbonate. Specifically, calcium chelators degrade the gel matrix by binding to the divalent calcium cations that are crosslinked with alginate, thereby disrupting the gel matrix and causing bead degradation to occur. Some common calcium chelators used for calcium alginate gel degradation are ethylenediamine tetraacetic acid (EDTA), ethylene glycol tetraacetic acid (EGTA), 1,2-bis(o-aminophenoxy)ethane-N,N,N',N'-tetraacetic acid (BAPTA), and citrate.[24,25] Interestingly, bicarbonate, the biomarker of metabolic alkalosis, also has the ability to bind to calcium to form calcium bicarbonate complexes. However, its binding activity was shown to be weak in comparison to citrate, exemplified by the slower degradation rate of the hydrogel beads with 1% calcium alginate and 20% dextran 6k in 50 mmol/L bicarbonate at 50 min compared with their fast degradation rate in 50 mmol/L citrate at 7 min as shown in Figure 3. The slow degradation rate of the hydrogel beads due to the bicarbonate is not ideal for the POC detection of metabolic alkalosis, which requires a rapid result. Therefore, in order to accelerate degradation of dextran hydrogel beads by bicarbonate, excess citric acid was added to samples containing bicarbonate to yield citrate via the following reaction.

$$3NaHCO_3 + C_6H_8O_7 \rightarrow 3Na^+ + C_6H_5O_7^{3-} + 3H_2O + 3CO_2$$

As a control, we also examined the degradation of hydrogel beads with 1% calcium alginate and 20% dextran 6k in 50 mmol/L citric acid. Additionally, as shown in Figure 2-3, citric acid by itself did not degrade the hydrogel beads over a 5 h period. Therefore, when using citric acid, the degradation rates of the hydrogel beads can be solely attributed to the formation of citrate, whose amount is directly correlated to the concentration of bicarbonate present in the patient's serum sample through the above reaction.

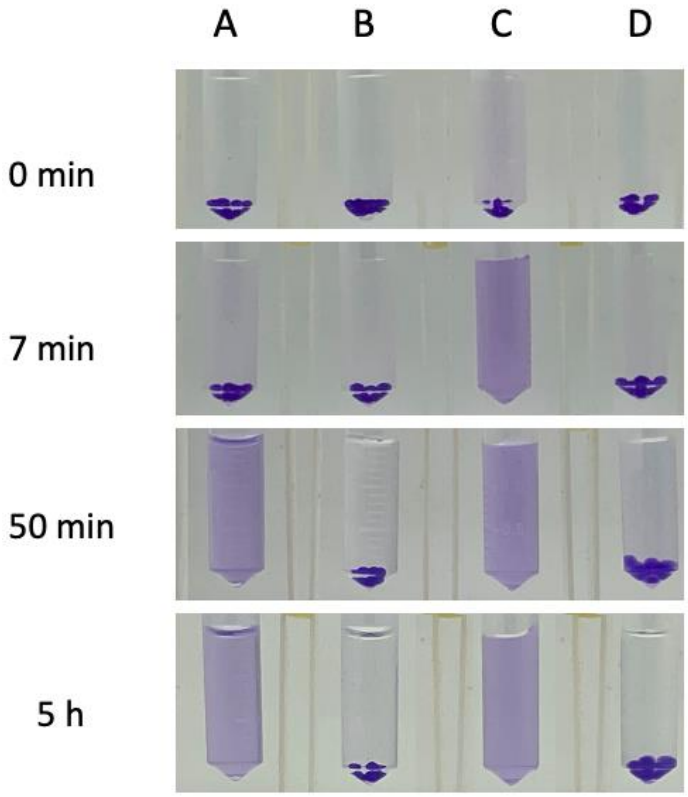

Figure 2-3. Degradation properties of hydrogel beads with 1% calcium alginate and 20% dextran 6k in (A) 50 mmol/L sodium bicarbonate in PBS, (B) 50 mmol/L citric acid in PBS, (C) 50 mmol/L sodium citrate in PBS, and (D) PBS.

2.3.4 Detection of bicarbonate in PBS

After separately testing the degradation properties of hydrogel beads with 1% calcium alginate and 20% dextran 6k in bicarbonate, citric acid, and citrate, their degradation due to the

bicarbonate-citric acid reaction was observed. Eight concentrations of sodium bicarbonate in PBS with an excess of citric acid were chosen to model varying concentrations of bicarbonate; concentrations below 30 mmol/L indicate the absence of metabolic alkalosis, concentrations at 30 mmol/L and above correspond to abnormal bicarbonate levels indicating metabolic alkalosis, and 0 mmol/L was the negative control. Figure 2-4 shows that degradation of the hydrogel beads was only observed in bicarbonate concentrations at 35 mmol/L and above. Specifically, the hydrogel beads in 50 mmol/L bicarbonate completely degraded in 37 min, followed by complete degradation in 45 mmol/L bicarbonate at 1 h 10 min. Complete degradation in 40 mmol/L bicarbonate only occurred at 11 h 35 min, and complete degradation of the hydrogel beads was not observed for bicarbonate concentrations of 35 mmol/L or below after 11 h 35 min. This trend proves that the degradation rates of the hydrogel beads can be directly correlated to the concentration of bicarbonate in PBS. However, the current degradation times were not ideal for POC diagnostics due to the long time-to-result for bicarbonate concentrations between 35 and 45 mmol/L.

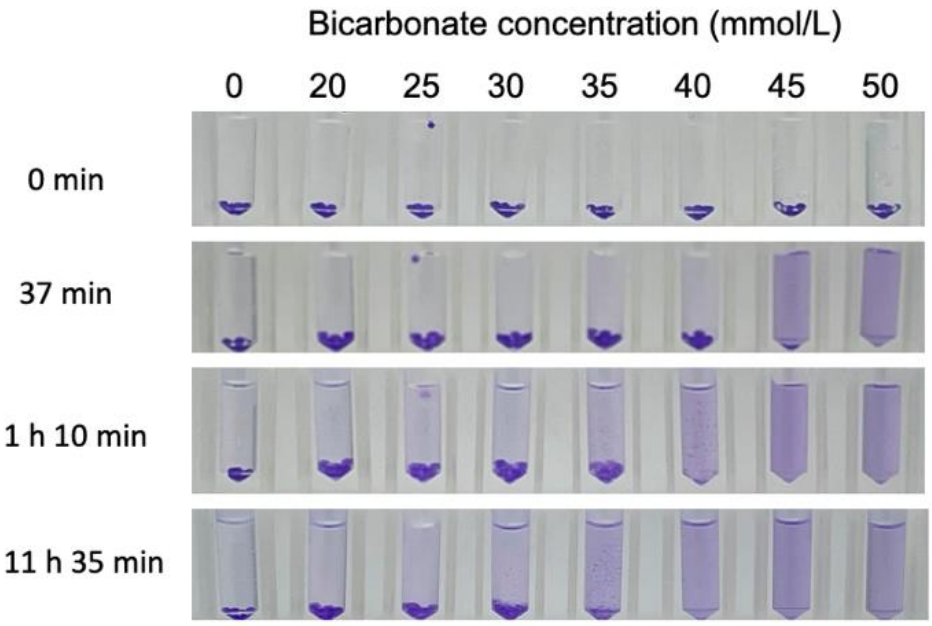

Figure 2-4. Degradation properties of hydrogel beads with 1% calcium alginate and 20% dextran 6k in varying concentrations of bicarbonate in PBS.

2.3.5 Gel bead optimization for the detection of bicarbonate

In order to design a rapid diagnostic assay, the degradation rates of the hydrogel beads needed to be accelerated. This was achieved by further lowering the percentage of calcium alginate in the gel beads. Faster degradation occurred with the lower calcium concentrations in the gel structure, since less citrate was required to completely chelate calcium cations and disassemble the gel matrix. However, hydrogels with a lower calcium alginate concentration exhibit less uniform bead morphology. For this reason, the concentration of dextran in the polymer solution was increased accordingly (20%, 30%, and 40%) while keeping the sodium alginate concentration constant (Figure 2-5A). Hydrogel beads with 1% calcium alginate and 50% dextran were not able to be synthesized due to the high viscosity of the polymer solution. For 0.2% and 0.4% calcium alginate hydrogel beads, significant increases in dextran concentrations showed little visible

improvement in bead morphology. In contrast, hydrogel beads with 0.6% and 0.8% calcium alginate and 40% dextran concentrations showed notable improvement in size and uniformity. Therefore, the degradation properties of hydrogel beads with 0.6% and 0.8% calcium alginate and 40% dextran were tested in varying levels of bicarbonate in PBS, as shown in Figures 2-5B and 2-5C, respectively. For hydrogel beads with 0.6% calcium alginate and 40% dextran, complete degradation was not observed for 0 and 20 mmol/L bicarbonate. For 25, 30, 35, and 40 mmol/L bicarbonate, full degradation was observed at 3 h, 1 h 24 min, 26 min, and 23 min, respectively. Lastly, degradation occurred at 14 min for both 45 and 50 mmol/L bicarbonate concentrations. For hydrogel beads with 0.8% calcium alginate and 40% dextran, complete degradation was not observed for 0, 20, and 25 mmol/L bicarbonate. Bicarbonate concentrations of 30, 35, 40, and 45 mmol/L showed complete degradation at 5 h 30 min, 2 h 4 min, 1 h 26 min, and 23 min, respectively. Lastly, degradation occurred at 19 min for 50 mmol/L bicarbonate. For both systems with reduced calcium alginate and 40% dextran (Figure 2-5), the degradation rates of the hydrogel beads substantially increased in comparison to hydrogel beads with 1% calcium alginate and 20% dextran (Figure 2-4). In addition, it was observed that both hydrogel bead systems with 40% dextran in elevated levels of bicarbonate from 35 mmol/L to 50 mmol/L showed much faster degradation rates compared to the concentrations close to or lower than the cut-off value typically used for metabolic alkalosis diagnosis (30 mmol/L). This notable finding allows for rapid and easy visual confirmation of the presence of elevated bicarbonate concentrations in a sample. Furthermore, since the hydrogel beads with 0.6% calcium alginate exhibited faster degradation properties than 0.8% calcium alginate, while maintaining good stability and morphology, these beads were further investigated. The stability and dye retention studies of hydrogel beads with 0.6% calcium alginate and 40% dextran 6k can be found in appendix (Figure A-1).

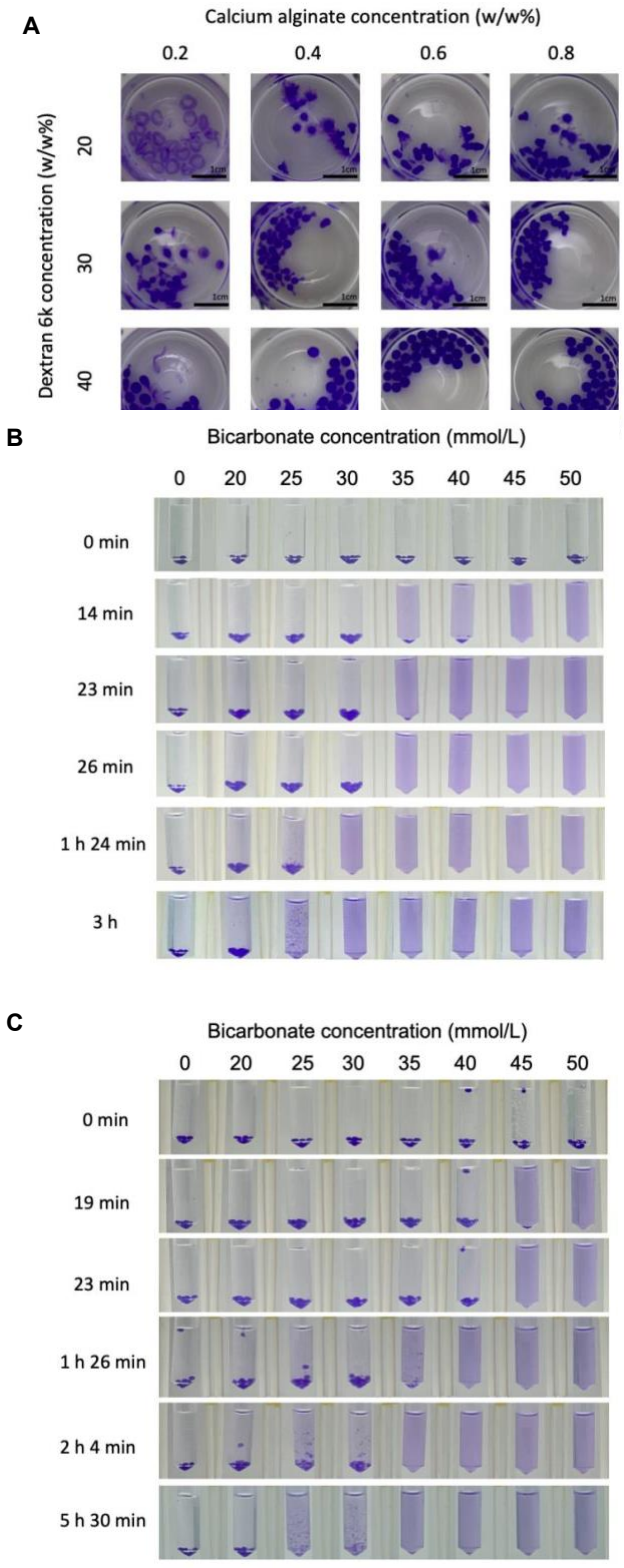

Figure 2-5. Optimization of CaAD hydrogel beads for the detection of abnormal concentrations of bicarbonate. (A) Synthesis of CaAD hydrogel beads with varying calcium alginate and dextran 6k

concentrations to optimize bead morphology for faster degradation rates. (B) Degradation of hydrogel beads with 0.6% calcium alginate and 40% dextran 6k in varying concentrations of bicarbonate in PBS over time. (C) Degradation of hydrogel beads with 0.8% calcium alginate and 40% dextran 6k in varying concentrations of bicarbonate in PBS over time.

2.3.6 Detection of bicarbonate in human serum

After achieving desirable degradation rates of the hydrogel beads with 0.6% calcium alginate and 40% dextran 6k in varying levels of bicarbonate in PBS, identical trials from Figure 2-5B were carried out using human serum samples spiked with bicarbonate to verify if our POC assay could function similarly in serum. As shown in Figure 2-6, the CaAD hydrogel beads at 50 mmol/L degrade completely in 10 min, followed by complete degradation in bicarbonate concentrations of 45, 40, and 35 mmol/L at 15 min, 20 min, and 54 min, respectively. The hydrogel beads in the lower bicarbonate concentrations of 30 and 25 mmol/L completely degraded in 2 h 12 min and 3 h 36 min, respectively. Lastly, the CaAD hydrogel beads in 0 and 20 mmol/L did not show significant degradation for 3 h 36 min. This degradation trend in human serum follows Figure 2-4C closely. Specifically, the degradation times of the CaAD hydrogel beads in the highest 3 bicarbonate concentrations were similar to those obtained in PBS. Moreover, although the degradation in 35 mmol/L bicarbonate was slowed down by half an hour relative to the PBS case, it still remained within the assay's one hour time frame. The degradation times in 30 and 25 mmol/L bicarbonate were also slower in comparison to the experiments in PBS (Figure 2-5B). These slight decreases in degradation times could potentially be attributed to components present in human serum. As the degradation rates of CaAD hydrogel beads in bicarbonate concentrations of 30 mmol/L and below were much slower than the degradation rates in the abnormal bicarbonate concentrations of 35 mmol/L and above, this system can be used to accurately detect for most

elevated bicarbonate levels in human serum ranging from 35 mmol/L to 50 mmol/L indicated by the fast degradation of the CaAD hydrogel beads and the release of the blue dye.

Overall, the degradation times of the CaAD hydrogel beads were successfully reproduced in human serum and proved to be well suited for diagnosis at the POC. The assay will be interpreted as follows: complete degradation of the CaAD hydrogel beads under one hour indicates abnormal concentrations of bicarbonate (35 mmol/L and above) in serum suggesting a high risk for metabolic alkalosis. At critically high concentrations of bicarbonate, the CaAD beads degrade in 20 min or less. In contrast, no significant degradation of the CaAD hydrogel beads occurred after an hour for serum levels of bicarbonate that are normal or near the cut-off value for metabolic alkalosis (30 mmol/L and below).

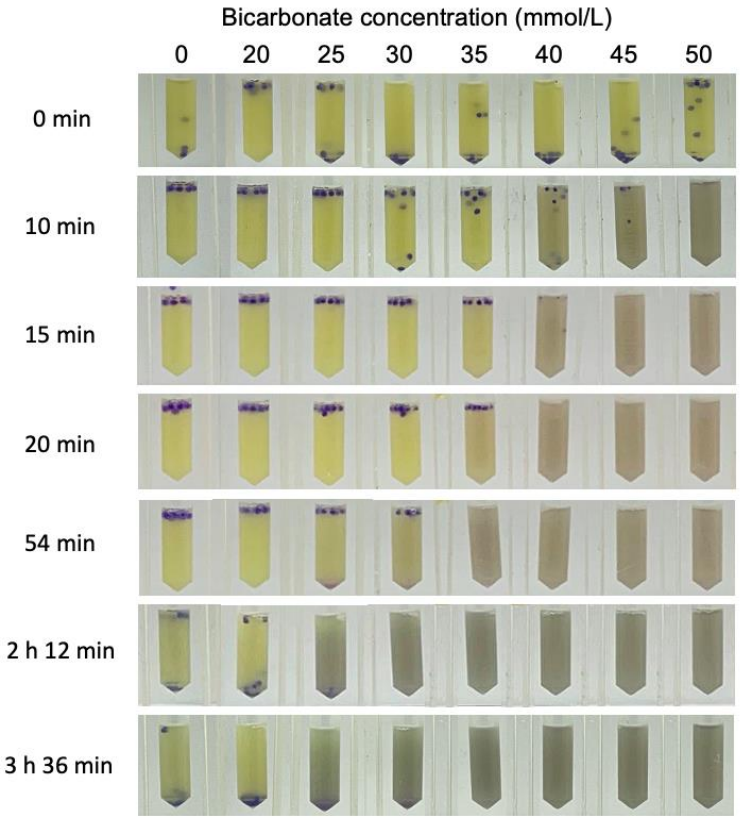

Figure 2-6. Degradation of hydrogel beads with 0.6% calcium alginate and 40% dextran 6k in varying concentrations of bicarbonate in human serum over time.

2.3.7 Device for the point of care

A POC-friendly device (Figure 2-7) was developed to aid in the detection of metabolic alkalosis in replacement of the lab equipment nutator. This device will be suitable for use in mobile clinics and resource-limited areas due to its small size, portability, low cost, low power requirements, and ease of use.

To test if the previous results attained in the nutator can be replicated with our device, degradation of hydrogel beads in 0, 30, 40, and 50 mmol/L bicarbonate in human serum were observed by placing the microcentrifuge tubes containing the CaAD hydrogel beads in the device. As shown in Figure 2-8, the hydrogel beads degraded at 10 min, 23 min, and 1 h 40 min in 50, 40, and 30 mmol/L bicarbonate samples, respectively. The CaAD hydrogel beads in the negative control (0 mmol/L bicarbonate) did not exhibit degradation within 6 h. These degradation times were close to those attained with the nutator (Figure 2-6) which were 10 min, 20 min, and 2 h 12 min for 50, 40, and 30 mmol/L bicarbonate concentrations, respectively. These findings validate the efficacy of the device for use in the rapid detection of metabolic alkalosis at the POC.

Figure 2-7. Device for the detection of metabolic alkalosis at the POC. A microcentrifuge tube holder was designed and attached to a rotating motor powered by a battery pack. A US penny is included for size comparison.

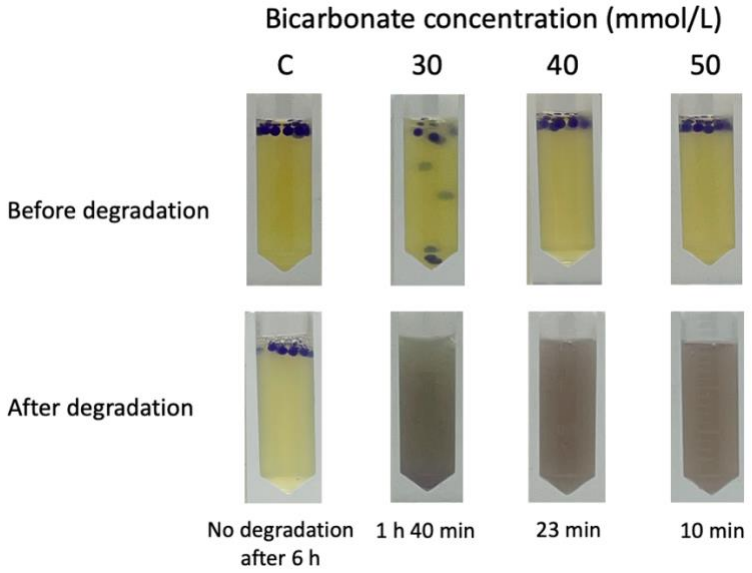

Figure 2-8. Degradation of hydrogel beads with 0.6% calcium alginate and 40% dextran 6k in varying bicarbonate concentrations in human serum using the POC diagnostic device.

2.4 Conclusion

We successfully developed a POC diagnostic assay using novel hydrogel beads for the detection of metabolic alkalosis. To our knowledge, we are the first group to study and apply CaAD hydrogel beads for diagnostics. Specifically, optimized hydrogel beads with 0.6% calcium alginate and 40% dextran 6k showed excellent properties for rapid detection of high concentrations of bicarbonate in both PBS and serum samples. The detection step involves the reaction of excess citric acid with bicarbonate, a marker for metabolic alkalosis functioning as the limiting reagent, to produce citrate. Citrate, a strong calcium chelator, rapidly disassembles the CaAD gels, and the degradation time was correlated with bicarbonate concentrations in serum. Our assay effectively detects high bicarbonate concentrations of 35 mmol/L and above, which indicates metabolic alkalosis, in less than an hour. More specifically, a serum bicarbonate concentration of 50 mmol/L was detected in as little as 10 min. Additionally, sodium bicarbonate concentrations of 45, 40, and 35 mmol/L were detected in 15, 20, and 54 min, respectively. In contrast, CaAD hydrogel beads in bicarbonate concentrations near the cut-off value of metabolic alkalosis (30 mmol/L and below) required well above an hour to show signs of degradation. Similar results were attained with our developed POC device. Thus, our inexpensive, rapid, and simple assay has the potential to be used in mobile clinics for the detection of metabolic alkalosis at the POC.

Chapter 3. Point-of-Care Detection of Biomarkers for Bacterial Infections

3.1 Introduction

Bacterial infections account for a wide range of global conditions and diseases every year. The common bacterial infection examples include but are not limited to those of the upper and lower respiratory tract, ear, throat, vagina, skin, urinary tract, brain and spinal cord, and blood, as well as a variety of sexually transmitted infections.[46] While most infections are curable with prompt antibiotics treatment, diseases that are untreated or mistreated can be life-threatening.[47] Moreover, bacteria may develop antibiotic resistance, and unfortunately, 'superbug' bacteria have appeared that are resistant towards multiple antibiotics. These 'superbug' bacteria include methicillin-resistant *Staphylococcus aureus* (MRSA) and various strains of *Escherichia coli* (*E.coli*).[48] In 2019, there were an estimated 4.95 million deaths in which antimicrobial resistant bacterial infection played a role, and an estimated 1.27 million deaths out of these cases were directly caused by drug-resistant bacterial infections.[49] Moreover, lower-income countries have the highest rates of death in relation to antimicrobial-resistant bacterial infections, with the highest percentage in Western sub-Saharan Africa at 27.3 deaths per 100,000 population.[49] To slow the emergence of this growing global health concern, the World Health Organization constructed a framework of interventions which included improving health systems and surveillances.

The current gold standard methods for diagnosing bacterial infection are bacteria culture and microscopy. These diagnostics are often expensive, and require trained personnel and laboratory settings which are not suitable for areas with limited resources. In addition, blood culture, the most common culture method in diagnosing infections, can miss at least 70% of infections as most bacteria do not enter the bloodstream,[51] leading to misdiagnosis and subsequent mistreatment. Mistreatment with antibiotics can also result in more bacteria with increased

resistance towards antibiotics on a global scale. Moreover, these tests usually have a long time-to-result, which is undesirable as prolonged diagnosis and lack of treatment will likely result in an increase in the severity of the disease and pose more risks in transmitting the bacterial infection to others. Therefore, there is a dire need for simple, rapid, and specific diagnostic assays for detecting bacterial infections to help physicians in their diagnosis and to ensure patients receive proper treatment in a timely manner to mitigate the spread of the disease, especially for those in resource-limited areas.

We drew inspiration from the recent work of the Schonherr group,[52] who developed a multiplex detection system using hydrogels consisting of chitosan chemically crosslinked with various colorimetric enzyme substrates. In their assay, the presence of a specific bacterial enzyme catalyzes a certain substate crosslinked in the gel matrix, thereby resulting in a colorimetric signal to indicate the presence of a particular bacterium. Taking advantage of hydrogel crosslinking and a colorimetric output to be indicative of bacterial infection, we developed a simpler and more user-friendly diagnostic assay using novel enzyme-responsive calcium alginate/EOPO hydrogel beads. We proposed that by mixing enzyme substrates with the polymer solution during bead synthesis, hybrid hydrogel beads with enzyme substrates incorporated into the gel matrix could be synthesized. Calcium alginate/EOPO hydrogel beads served as the foundation for these gel beads due to their advantages shown in Chapter 2, and the enzyme substrates were added to this foundation. The hybrid beads with encapsulated dye molecules would allow rapid, user-friendly, and specific detection of bacteria indicated by the degradation of the gel matrix and release of a colorimetric dye resulting from a bacteria enzyme catalyzing substrates incorporated with the gel matrix.

3.2 Materials and Methods

3.2.1 Preparation of the polymer solution and gelation bath

All reagents and materials were purchased from Sigma-Aldrich unless otherwise noted. To prepare the polymer solution, a 1.5% w/w sodium alginate solution containing 15% w/w EOPO and various concentrations of enzyme substrates, including pullulan (Tokyo Chemical Industry Co. Japan), carrageenan, starch, gelatin, chitosan, agarose (Fisher Scientific, Hampton, NH), and cellulose, were prepared in deionized water. Additionally, 0.25 mg of Coomassie Brilliant Blue G-250 dye in deionized water was added per 1 mL of polymer solution for hydrogel visualization and enzyme detection. For the salt gelation bath, a 1.5% w/w calcium chloride solution was prepared in deionized water.

3.2.2 Hydrogel synthesis

As shown in Figure 3-1, a simple experimental setup was employed to synthesize the hybrid hydrogel beads. Briefly, a 1 mL Luer lock syringe containing the polymer solution was positioned vertically with its attached 30G needle tip and suspended approximately 10 cm above a glass scintillation vial containing the gelation bath. The syringe needed to be a certain height above the scintillation vial to ensure polymer droplets hit the gelation bath at a speed fast enough to allow for full immersion in the bath. This was to ensure uniform crosslinking during hydrogel formation to generate beads of the desired spherical geometry. The syringe plunger was gently pressed to continuously dispense polymer droplets. After the polymer solution was fully dispensed, the hydrogel beads were left to incubate in the gelation bath at room temperature for at least 1 h to allow for completion of the crosslinking reaction, further stabilizing the hydrogel matrix. After the incubation period, the hydrogel beads were collected and washed with deionized water to remove

excess calcium chloride ions. Pictures were taken in a controlled lighting environment with an iPhone 12 camera. All hydrogel beads were stored in water at room temperature.

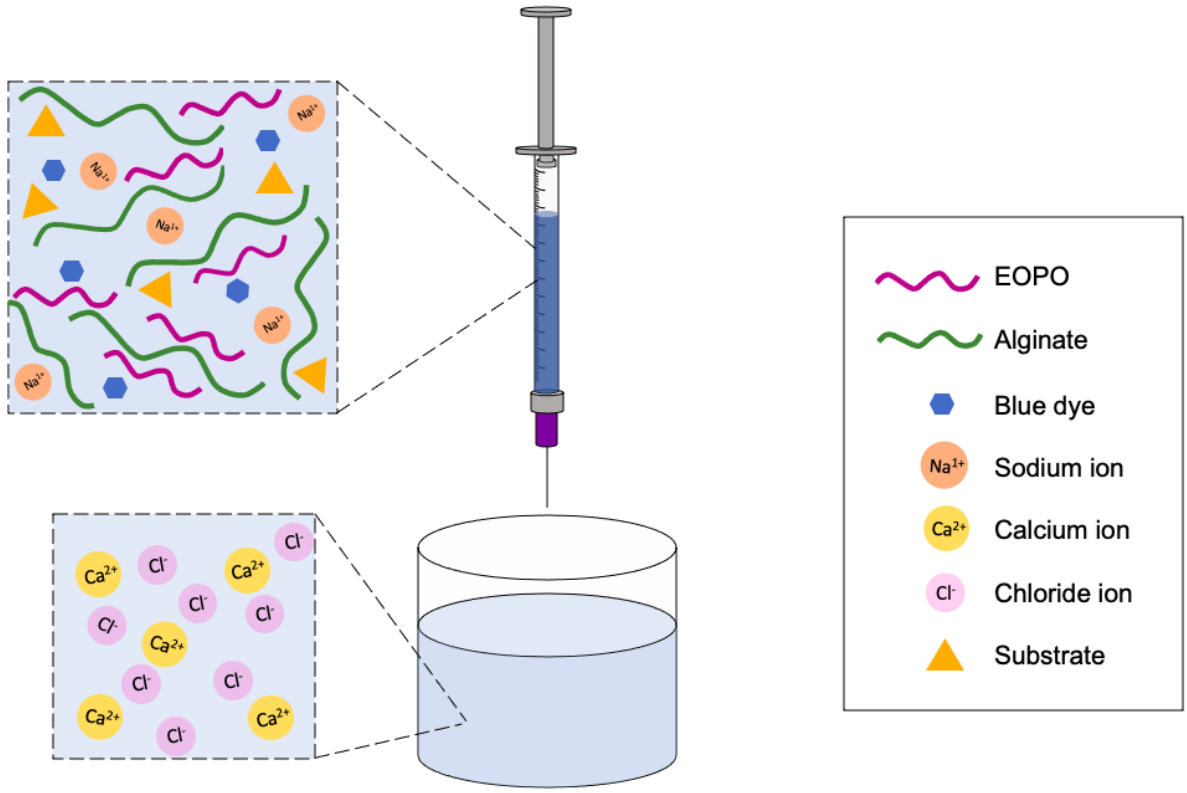

Figure 3-1 Schematic of the ionic crosslinking set up for hybrid hydrogel bead synthesis. Briefly, a polymer solution containing sodium alginate, EOPO, enzyme substrates, and dye was dispensed dropwise into a gelation bath containing calcium chloride, allowing for the complexation between alginate polymers and calcium ions to form a spherical gel matrix instantaneously.

3.2.3 Detection of bacterial enzymes

Varying concentrations of bacterial enzymes including α-amylase, cellulase, and trypsin were prepared in filtered ultrapure water (FUP), PBS, and 0.1M Tris buffer (pH 7.5). For the degradation studies, hydrogel beads were incubated in 1 mL of an enzyme solution in a 1.7 mL microcentrifuge tube placed on a nutator at room temperature. Pictures were taken to record the dye release and hydrogel bead degradation over time with an iPhone 12 camera.

3.3 Results and Discussion

3.3.1 Hybrid hydrogel beads for the detection of bacteria

Hybrid hydrogel beads with the incorporation of various enzyme substrates (carrageenan, starch, gelatin, chitosan, agarose, and cellulose) were synthesized, and their morphologies were studied. Table 3-1 shows a list of bacteria enzymes and substrates studied.

Table 3-1 Enzymes and substrates used in this study

Substrate	**Enzyme that degrades the substrate**	**Bacteria that produce the enzyme**
Cellulose	Cellulase	*Pseudomonas fluorescens, Bacillus subtilis, E. coli,* and *Serratia marcescens*.[53]
Chitosan	Chitosanase	*Bacillus* sp., *Pedobacter* sp., and *Streptomyces* sp.[54]
Gelatin	Trypsin	*Bacillus cereus*, *Enterococcus mundtii*, *Enterococcus gallinarum*, and *Staphylococcus xylosus*.[55]
Agarose	Agarase	*Pseudomonas* sp. and *Vibrio* sp.[56]
Carrageenan	Carrageenase	*Pseudoalteromonas carrageenovora* and *Alteromonas fortis*[57]
Pullulan and starch	α-Amylase	*Bacillus amyloliquefaciens, Bacillus licheniformis*, and *Bacillus stearothermophilus*[58]

The hydrogel beads in a diagnostic assay should be monodisperse and spherical for several reasons. Uniform spherical beads ensure consistent degradation rates for each bead due to having the same surface area in contact with the environment. Their uniform sizes also allow for encapsulation of equal volume of dye, allowing for consistent dye release for the detection by the naked eye. They are also relatively easy to synthesize. Lastly, their small volume sizes allow for smaller patient sample volumes to be used.

3.3.2 Calcium alginate/EOPO/gelatin hydrogel beads

3.3.2.1 Morphology, stability, and dye release properties

Hydrogel beads with the incorporation of gelatin were successfully synthesized as shown in Figure 3-2. The hydrogel beads demonstrated uniform sizes; however, they were flat and their shapes were not uniform nor spherical. Hydrogel beads made with 1.8% gelatin were slightly larger in size than hydrogel beads with 0.9% gelatin, but they both demonstrated good stability and strong dye retention after 7 days.

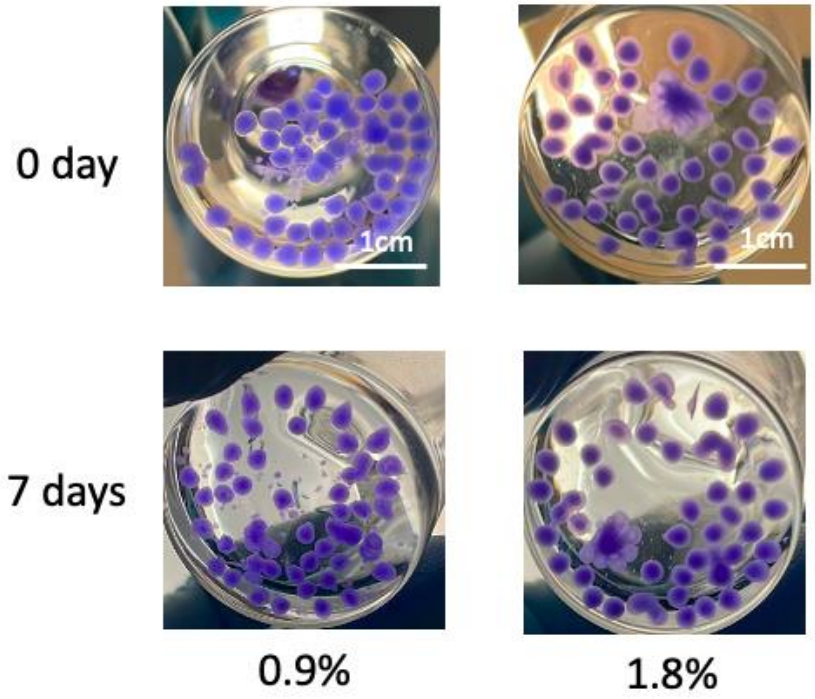

Figure 3-2 Morphology, stability, and dye release studies of 1.5% calcium alginate/15% EOPO/gelatin hydrogel beads consisting of different concentrations of gelatin. (Left) 0.9% gelatin. (Right) 1.8% gelatin.

3.3.2.2 Degradation properties in the presence of trypsin

With the incubation of 1.5% calcium alginate/15% EOPO/1.8% gelatin hydrogel beads in 1 mg/mL trypsin in PBS, the beads showed slight gel degradation at 7 min followed by complete degradation at 13 min, whereas the negative control did not achieve complete degradation at 80

min, as shown in Figure 3-3. This result demonstrated that trypsin plays a significant role in the degradation of the gelatin-incorporated hydrogel beads. However, the beads demonstrated weaker stability in PBS compared to water as two out of the three beads in the negative control had undergone degradation after 80 min.

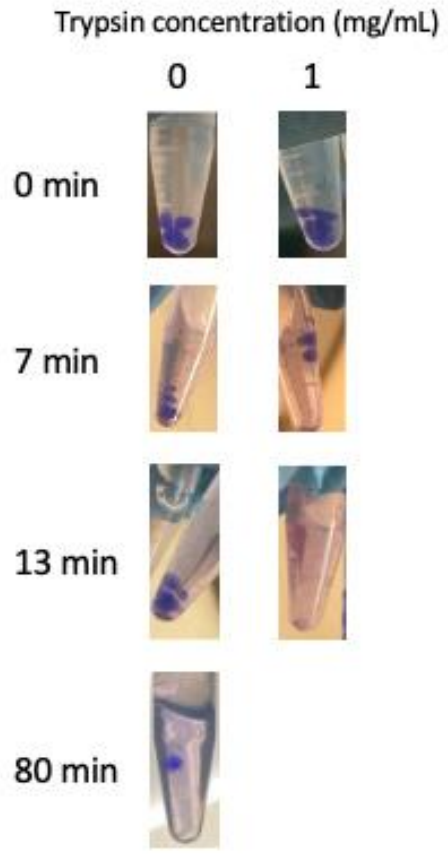

Figure 3-3 Degradation properties of 1.5% calcium alginate/15% EOPO/1.8% gelatin hydrogel beads in varying concentrations of trypsin in PBS.

3.3.3 Calcium alginate/EOPO/pullulan hydrogel beads

3.3.3.1 Morphology, stability, and dye release properties

Although the hydrogel beads synthesized with pullulan appeared uniform in size, they exhibited tear drop shapes and were not spherical (Figure 3-4). Inconsistent and more transparent gel beads were synthesized at the start of syringe extrusion, while smaller beads were consistently

synthesized after this initial period. While the beads demonstrated good stability in water as they maintained their original morphologies after 4 days, there was slight degradation of the gel demonstrated by the slightly milky solution at day 4, which could potentially be due to degraded gel pieces. In addition, there was some observable dye release at day 1.

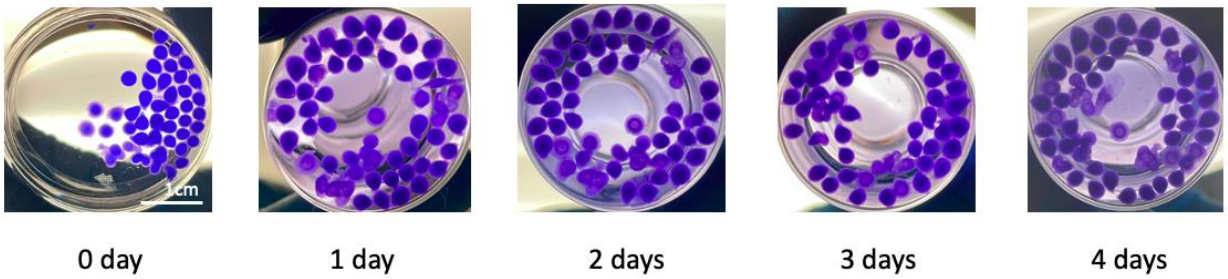

Figure 3-4 Morphology, stability, and dye release studies of 1.5% calcium alginate/15% EOPO/0.75% pullulan hydrogel beads.

3.3.3.2 Degradation properties in the presence of α-amylase

With the incubation of 1.5% calcium alginate/15% EOPO/0.75% pullulan hydrogel beads in various concentrations of α-amylase in 0.1M Tris buffer, beads in both 3 mg/mL and 5 mg/mL α-amylase solutions demonstrated similar degradation rates in comparison to the negative control. Specifically, beads in both concentrations started degrading at 30 min and achieved complete degradation at 3 h, with the beads in the negative control exhibiting no degradation at 3 h (Figure 3-5). This result demonstrated that α-amylase does indeed play a significant role in the degradation of the pullulan-incorporated hydrogel beads. However, increasing the concentration from 3 to 5 mg/mL of α-amylase did not seem to influence the degradation rates.

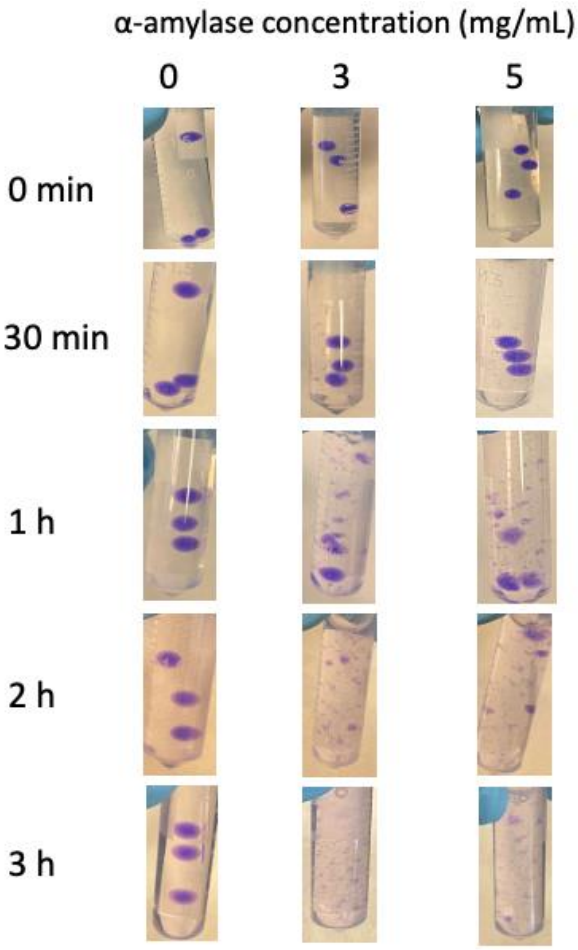

Figure 3-5 Degradation properties of 1.5% calcium alginate/15% EOPO/0.75% pullulan hydrogel beads in varying concentrations of α-amylase in 0.1M Tris buffer.

3.3.4 Calcium alginate/EOPO/starch hydrogel beads

3.3.4.1 Morphology, stability, and dye release properties

Hydrogel beads synthesized with starch were spherical, but their sizes were not completely uniform as shown in Figure 3-6. Inconsistent, larger, and more transparent gel beads were synthesized at the start of syringe extrusion, while smaller beads were consistently synthesized after this initial period. Figure 3-6 also shows that the beads were fairly stable in water after 5 days as each bead retained its original morphology. There was, however, some slight degradation of the gel after 5 days demonstrated by the milky color in the solution.

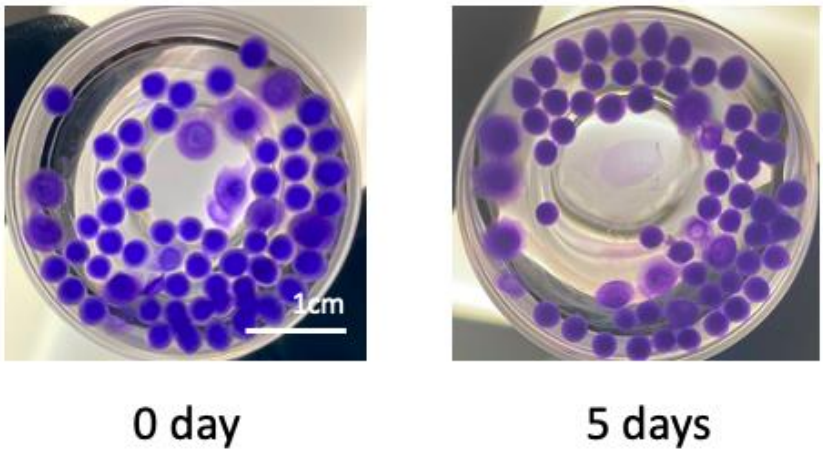

Figure 3-6 Morphology, stability, and dye release studies of calcium 1.5% alginate/15% EOPO/1.5% starch hydrogel beads.

3.3.4.2 Degradation properties in the presence of α-amylase

The 1.5% calcium alginate/15% EOPO/1.5% starch hydrogel beads were incubated in various concentrations of α-amylase in 0.1M Tris buffer. As shown in Figure 3-7, there was some degree of correlation between α-amylase concentration and gel bead degradation rate. Specifically, at 1 h after incubation, hydrogel beads in 3 mg/mL showed slight degradation. At 2 h, beads in 1.5 mg/mL and 2 mg/mL α-amylase concentrations showed slight degradation, and beads in 3 mg/mL α-amylase showed relatively more degradation. At 4 h, all beads in the presence of α-amylase showed substantial degradation, whereas beads in the negative control showed minimal degradation as indicated by their intact spherical shapes. While this result demonstrated that higher α-amylase concentrations increased bead degradation rates, the degradation times were still too long which is undesirable for a point-of-care test. Future experiments with higher α-amylase concentrations could be performed to further analyze the effect of α-amylase concentration.

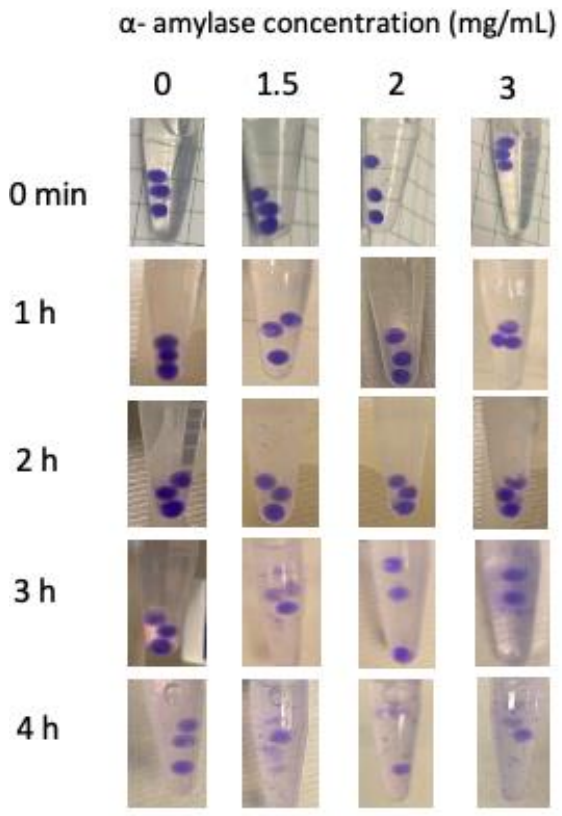

Figure 3-7 Degradation properties of 1.5% alginate/15% EOPO/1.5% starch hydrogel beads in varying concentrations of α-amylase in 0.1M Tris buffer.

3.3.5 Calcium alginate/EOPO/cellulose hydrogel beads

3.3.5.1 Morphology, stability, and dye release properties

As shown in Figure 3-8, the hydrogel beads synthesized with cellulose appeared to be spherical and uniform in size, while also having more transparent and thicker gel shells than the rest of the hydrogel bead systems. Regardless of the transparency of the gel, the beads demonstrated excellent stability in water after 5 days. In addition, the gel beads had excellent retention of dye after 5 days. The concentration of cellulose also did not seem to have an apparent effect on bead morphology.

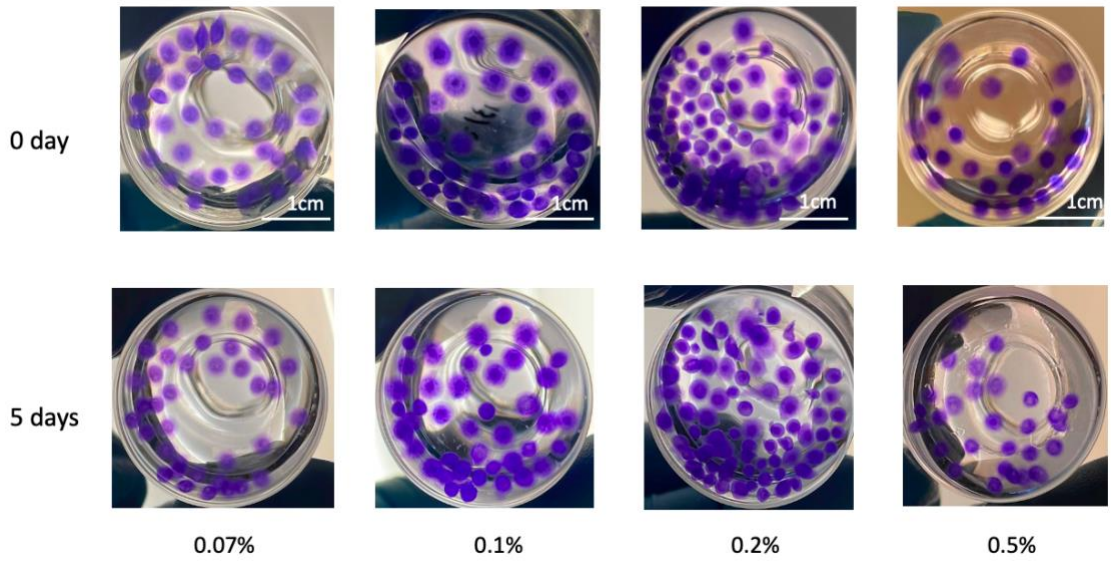

Figure 3-8 Morphology, stability, and dye release studies of calcium 1.5% alginate/15% EOPO/cellulose hydrogel beads consisting of different concentrations of cellulose. From left to right, the hydrogel beads consisted of 0.07%, 0.1%, 0.2%, and 0.5% cellulose.

3.3.5.2 Degradation properties in the presence of cellulase

Degradation was unfortunately not observed for cellulose-incorporated hydrogel beads in 10 mg/mL cellulase in FUP, PBS, and 0.1M Tris buffer (data not shown).

3.3.6 Additional thoughts on calcium alginate/EOPO/substrates hydrogel beads

Calcium alginate/EOPO/carrageenan hydrogel beads were successfully synthesized. Their morphology, stability, and dye release studies can be found in Figure A-2 in the Appendix. Calcium alginate/EOPO/agarose and calcium alginate/EOPO/chitosan hydrogel beads were not successfully synthesized.

3.4 Conclusion

To our knowledge, we are the first group to have successfully synthesized calcium alginate hydrogel beads with the incorporation of an additional nonionic polymer and a bacterial enzyme

substrate, which simultaneously improved bead morphology and allowed for the detection of bacterial enzymes. By incorporating enzyme substrates in the hydrogel bead synthesis procedure, bead degradation and release of dye would indicate the presence of bacterial enzymes, which could be used in the future to diagnose bacterial infection. We were able to achieve gel-sol degradation of the hydrogel beads in response to various bacterial enzymes. Specifically, the beads comprised of calcium alginate/EOPO/gelatin, calcium alginate/EOPO/pullulan, and calcium alginate/EOPO/starch demonstrated a gel-sol degradation response towards 1 mg/mL trypsin in PBS, 3 to 5 mg/mL α-amylase in 0.1M Tris buffer, and 1.5 to 3 mg/mL α-amylase in 0.1M Tris buffer, respectively.

These gel-sol degradation times could be further shortened by optimizing the hydrogel beads through manipulating the concentrations of calcium alginate, EOPO, and enzyme substrate. The degradation process in this chapter also does not involve inverting or heating the tube, but a simple point-of-care device can be built to incorporate inversion and heat during degradation to achieve shorter degradation times.

Moving forward, the calcium alginate/EOPO/enzyme substrate hydrogel beads can also be developed into a multiplex detection system where different hydrogel beads can contain different enzyme substrates and dyes. In so doing, the degradation and release of a particular dye color would indicate the presence of a specific bacterium.

References

(1) Chai, Q.; Jiao, Y.; Yu, X. Hydrogels for Biomedical Applications: Their Characteristics and the Mechanisms behind Them. *Gels* **2017**, *3* (1), 6. https://doi.org/10.3390/gels3010006.

(2) Stile, R. A.; Healy, K. E. Thermo-Responsive Peptide-Modified Hydrogels for Tissue Regeneration. *Biomacromolecules* **2001**, *2* (1), 185–194. https://doi.org/10.1021/bm0000945.

(3) Petersen, O. W.; Rønnov-Jessen, L.; Howlett, A. R.; Bissell, M. J. Interaction with Basement Membrane Serves to Rapidly Distinguish Growth and Differentiation Pattern of Normal and Malignant Human Breast Epithelial Cells. *Proc. Natl. Acad. Sci. U.S.A.* **1992**, *89* (19), 9064–9068. https://doi.org/10.1073/pnas.89.19.9064.

(4) Chowdhury, F.; Li, Y.; Poh, Y.-C.; Yokohama-Tamaki, T.; Wang, N.; Tanaka, T. S. Soft Substrates Promote Homogeneous Self-Renewal of Embryonic Stem Cells via Downregulating Cell-Matrix Tractions. *PLoS ONE* **2010**, *5* (12), e15655. https://doi.org/10.1371/journal.pone.0015655.

(5) Caliari, S. R.; Burdick, J. A. A Practical Guide to Hydrogels for Cell Culture. *Nat Methods* **2016**, *13* (5), 405–414. https://doi.org/10.1038/nmeth.3839.

(6) Mancha Sánchez, E.; Gómez-Blanco, J. C.; López Nieto, E.; Casado, J. G.; Macías-García, A.; Díaz Díez, M. A.; Carrasco-Amador, J. P.; Torrejón Martín, D.; Sánchez-Margallo, F. M.; Pagador, J. B. Hydrogels for Bioprinting: A Systematic Review of Hydrogels Synthesis, Bioprinting Parameters, and Bioprinted Structures Behavior. *Front. Bioeng. Biotechnol.* **2020**, *8*, 776. https://doi.org/10.3389/fbioe.2020.00776.

(7) Klotz, B. J.; Gawlitta, D.; Rosenberg, A. J. W. P.; Malda, J.; Melchels, F. P. W. Gelatin-Methacryloyl Hydrogels: Towards Biofabrication-Based Tissue Repair. *Trends in Biotechnology* **2016**, *34* (5), 394–407. https://doi.org/10.1016/j.tibtech.2016.01.002.

(8) Qiu, Y.; Park, K. Environment-Sensitive Hydrogels for Drug Delivery. *Advanced Drug Delivery Reviews* **2001**, *53* (3), 321–339. https://doi.org/10.1016/S0169-409X(01)00203-4.

(9) Buwalda, S. J.; Vermonden, T.; Hennink, W. E. Hydrogels for Therapeutic Delivery: Current Developments and Future Directions. *Biomacromolecules* **2017**, *18* (2), 316–330. https://doi.org/10.1021/acs.biomac.6b01604.

(10) Jia, Z.; Müller, M.; Le Gall, T.; Riool, M.; Müller, M.; Zaat, S. A. J.; Montier, T.; Schönherr, H. Multiplexed Detection and Differentiation of Bacterial Enzymes and Bacteria by Color-Encoded Sensor Hydrogels. *Bioactive Materials* **2021**, *6* (12), 4286–4300. https://doi.org/10.1016/j.bioactmat.2021.04.022.

(11) Barclay, R. A.; Akhrymuk, I.; Patnaik, A.; Callahan, V.; Lehman, C.; Andersen, P.; Barbero, R.; Barksdale, S.; Dunlap, R.; Goldfarb, D.; Jones-Roe, T.; Kelly, R.; Kim, B.; Miao, S.; Munns, A.; Munns, D.; Patel, S.; Porter, E.; Ramsey, R.; Sahoo, S.; Swahn, O.; Warsh, J.; Kehn-Hall, K.; Lepene, B. Hydrogel Particles Improve Detection of SARS-CoV-2 RNA from Multiple Sample Types. *Sci Rep* **2020**, *10* (1), 22425. https://doi.org/10.1038/s41598-020-78771-8.

(12) Hafezi, M.; Nouri Khorasani, S.; Zare, M.; Esmaeely Neisiany, R.; Davoodi, P. Advanced Hydrogels for Cartilage Tissue Engineering: Recent Progress and Future Directions. *Polymers* **2021**, *13* (23), 4199. https://doi.org/10.3390/polym13234199.

(13) Lee, J. C.; Pereira, C. T.; Ren, X.; Huang, W.; Bischoff, D.; Weisgerber, D. W.; Yamaguchi, D. T.; Harley, B. A.; Miller, T. A. Optimizing Collagen Scaffolds for Bone Engineering: Effects of Cross-Linking and Mineral Content on Structural Contraction and Osteogenesis. *Journal of Craniofacial Surgery* **2015**, *26* (6), 1992–1996. https://doi.org/10.1097/SCS.0000000000001918.

(14) *Chemistry of Crosslinking*. THermoFisher Scientific. https://www.thermofisher.com/us/en/home/life-science/protein-biology/protein-biology-learning-center/protein-biology-resource-library/pierce-protein-methods/chemistry-crosslinking.html.

(15) George, J.; Hsu, C.-C.; Nguyen, L. T. B.; Ye, H.; Cui, Z. Neural Tissue Engineering with Structured Hydrogels in CNS Models and Therapies. *Biotechnology Advances* **2020**, *42*, 107370. https://doi.org/10.1016/j.biotechadv.2019.03.009.

(16) Zhang, H.; Zhang, F.; Wu, J. Physically Crosslinked Hydrogels from Polysaccharides Prepared by Freeze–Thaw Technique. *Reactive and Functional Polymers* **2013**, *73* (7), 923–928. https://doi.org/10.1016/j.reactfunctpolym.2012.12.014.

(17) Ermis, M.; Calamak, S.; Calibasi Kocal, G.; Guven, S.; Durmus, N. G.; Rizvi, I.; Hasan, T.; Hasirci, N.; Hasirci, V.; Demirci, U. Hydrogels as a New Platform to Recapitulate the Tumor Microenvironment. In *Handbook of Nanomaterials for Cancer Theranostics*; Elsevier, 2018; pp 463–494. https://doi.org/10.1016/B978-0-12-813339-2.00015-3.

(18) parhi, R. Cross-Linked Hydrogel for Pharmaceutical Applications: A Review. *Adv Pharm Bull* **2017**, *7* (4), 515–530. https://doi.org/10.15171/apb.2017.064.

(19) Berger, J.; Reist, M.; Mayer, J. M.; Felt, O.; Peppas, N. A.; Gurny, R. Structure and Interactions in Covalently and Ionically Crosslinked Chitosan Hydrogels for Biomedical

Applications. *European Journal of Pharmaceutics and Biopharmaceutics* **2004**, *57* (1), 19–34. https://doi.org/10.1016/S0939-6411(03)00161-9.

(20) Vinchhi, P.; Rawal, S. U.; Patel, M. M. Biodegradable Hydrogels. In *Drug Delivery Devices and Therapeutic Systems*; Elsevier, 2021; pp 395–419. https://doi.org/10.1016/B978-0-12-819838-4.00012-2.

(21) Skjåk-Bræk, G.; Draget, K. I. Alginates. In *Polymer Science: A Comprehensive Reference*; Elsevier, 2012; pp 213–220. https://doi.org/10.1016/B978-0-444-53349-4.00261-2.

(22) Song, E.-H.; Shang, J.; Ratner, D. M. Polysaccharides. In *Polymer Science: A Comprehensive Reference*; Elsevier, 2012; pp 137–155. https://doi.org/10.1016/B978-0-444-53349-4.00246-6.

(23) Plazinski, W. Molecular Basis of Calcium Binding by Polyguluronate Chains. Revising the Egg-Box Model. *J. Comput. Chem.* **2011**, *32* (14), 2988–2995. https://doi.org/10.1002/jcc.21880.

(24) Dixon, S. J.; Lemberg, K. M.; Lamprecht, M. R.; Skouta, R.; Zaitsev, E. M.; Gleason, C. E.; Patel, D. N.; Bauer, A. J.; Cantley, A. M.; Yang, W. S.; Morrison, B.; Stockwell, B. R. Ferroptosis: An Iron-Dependent Form of Nonapoptotic Cell Death. *Cell* **2012**, *149* (5), 1060–1072. https://doi.org/10.1016/j.cell.2012.03.042.

(25) Keowmaneechai, E.; McClements, D. J. Influence of EDTA and Citrate on Physicochemical Properties of Whey Protein-Stabilized Oil-in-Water Emulsions Containing $CaCl_2$. *J. Agric. Food Chem.* **2002**, *50* (24), 7145–7153. https://doi.org/10.1021/jf020489a.

(26) Doumèche, B.; Picard, J.; Larreta-Garde, V. Enzyme-Catalyzed Phase Transition of Alginate Gels and Gelatin−Alginate Interpenetrated Networks. *Biomacromolecules* **2007**, *8* (11), 3613–3618. https://doi.org/10.1021/bm700767u.

(27) Gurikov, P.; Smirnova, I. Non-Conventional Methods for Gelation of Alginate. *Gels* **2018**, *4* (1), 14. https://doi.org/10.3390/gels4010014.

(28) Lee, B.-B.; Ibrahim, R.; Chu, S.-Y.; Zulkifli, N. A.; Ravindra, P. Alginate Liquid Core Capsule Formation Using the Simple Extrusion Dripping Method. *Journal of Polymer Engineering* **2015**, *35* (4), 311–318. https://doi.org/10.1515/polyeng-2014-0174.

(29) *Ionic crosslinking*. Labster Theory. https://theory.labster.com/ionic-crosslinking/.

(30) Naseri, M.; Ziora, Z. M.; Simon, G. P.; Batchelor, W. ASSURED-compliant Point-of-care Diagnostics for the Detection of Human Viral Infections. *Reviews in Medical Virology* **2022**, *32* (2). https://doi.org/10.1002/rmv.2263.

(31) *Point of Care Diagnostics Market by Product (Glucose Monitoring Products, Infectious Diseases Testing Products, Pregnancy & Fertility Testing Products, Cardiometabolic Testing Products, Coagulation Testing Products, Others); by Mode of Purchase (Over the Counter, Prescriptions); by End User (Hospitals & Clinics, Homecare & DTC, Others); by Region : Global Forecasts 2021 To 2027*; 248; All the Research, 2021.

(32) Gunatilake, U. B.; Garcia-Rey, S.; Ojeda, E.; Basabe-Desmonts, L.; Benito-Lopez, F. TiO_2 Nanotubes Alginate Hydrogel Scaffold for Rapid Sensing of Sweat Biomarkers: Lactate and Glucose. *ACS Appl. Mater. Interfaces* **2021**, *13* (31), 37734–37745. https://doi.org/10.1021/acsami.1c11446.

(33) Zhao, L.; Yin, S.; Ma, Z. Ca $^{2+}$ -Triggered PH-Response Sodium Alginate Hydrogel Precipitation for Amplified Sandwich-Type Impedimetric Immunosensor of Tumor Marker. *ACS Sens.* **2019**, *4* (2), 450–455. https://doi.org/10.1021/acssensors.8b01465.

(34) Yin, S.; Ma, Z. "Smart" Sensing Interface for the Improvement of Electrochemical Immunosensor Based on Enzyme-Fenton Reaction Triggered Destruction of Fe3+ Cross-Linked Alginate Hydrogel. *Sensors and Actuators B: Chemical* **2019**, *281*, 857–863. https://doi.org/10.1016/j.snb.2018.11.030.

(35) Al Sulaiman, D.; Chang, J. Y. H.; Bennett, N. R.; Topouzi, H.; Higgins, C. A.; Irvine, D. J.; Ladame, S. Hydrogel-Coated Microneedle Arrays for Minimally Invasive Sampling and Sensing of Specific Circulating Nucleic Acids from Skin Interstitial Fluid. *ACS Nano* **2019**, *13* (8), 9620–9628. https://doi.org/10.1021/acsnano.9b04783.

(36) Zhang, Y. S.; Khademhosseini, A. Advances in Engineering Hydrogels. *Science* **2017**, *356* (6337), eaaf3627. https://doi.org/10.1126/science.aaf3627.

(37) Zhu, Y.; Zhang, J.; Song, J.; Yang, J.; Du, Z.; Zhao, W.; Guo, H.; Wen, C.; Li, Q.; Sui, X.; Zhang, L. A Multifunctional Pro-Healing Zwitterionic Hydrogel for Simultaneous Optical Monitoring of PH and Glucose in Diabetic Wound Treatment. *Adv. Funct. Mater.* **2020**, *30* (6), 1905493. https://doi.org/10.1002/adfm.201905493.

(38) Puchberger-Enengl, D.; Krutzler, C.; Keplinger, F.; Vellekoop, M. J. Single-Step Design of Hydrogel-Based Microfluidic Assays for Rapid Diagnostics. *Lab Chip* **2014**, *14* (2), 378–383. https://doi.org/10.1039/C3LC50944C.

(39) Lee, K. Y.; Mooney, D. J. Alginate: Properties and Biomedical Applications. *Progress in Polymer Science* **2012**, *37* (1), 106–126. https://doi.org/10.1016/j.progpolymsci.2011.06.003.

(40) Abd El-Ghaffar, M. A.; Hashem, M. S.; El-Awady, M. K.; Rabie, A. M. PH-Sensitive Sodium Alginate Hydrogels for Riboflavin Controlled Release. *Carbohydrate Polymers* **2012**, *89* (2), 667–675. https://doi.org/10.1016/j.carbpol.2012.03.074.

(41) Kobašlija, M.; McQuade, D. T. Removable Colored Coatings Based on Calcium Alginate Hydrogels. *Biomacromolecules* **2006**, *7* (8), 2357–2361. https://doi.org/10.1021/bm060341q.

(42) Hoffman, A. S. Applications of Thermally Reversible Polymers and Hydrogels in Therapeutics and Diagnostics. *Journal of Controlled Release* **1987**, *6* (1), 297–305. https://doi.org/10.1016/0168-3659(87)90083-6.

(43) Soifer, J. T.; Kim, H. T. Approach to Metabolic Alkalosis. *Emergency Medicine Clinics of North America* **2014**, *32* (2), 453–463. https://doi.org/10.1016/j.emc.2014.01.005.

(44) Galla, J. H. Metabolic Alkalosis. *JASN* **2000**, *11* (2), 369–375. https://doi.org/10.1681/ASN.V112369.

(45) Mahdi, M. H.; Diryak, R.; Kontogiorgos, V.; Morris, G. A.; Smith, A. M. In Situ Rheological Measurements of the External Gelation of Alginate. *Food Hydrocolloids* **2016**, *55*, 77–80. https://doi.org/10.1016/j.foodhyd.2015.11.002.

(46) Jennifer Huizen. *What are the symptoms of a bacterial infection?*. MedicalNewsToday. https://www.medicalnewstoday.com/articles/bacterial-infection-symptoms.

(47) *Bacterial infections*. HealthDirect. https://www.healthdirect.gov.au/bacterial-infections#:~:text=Most%20bacterial%20infections%20can%20be,that%20is%20causing%20the%20infection.

(48) *Antibiotic resistanc*. HealthDirect. https://www.healthdirect.gov.au/antibiotic-resistance.

(49) Thompson, T. The Staggering Death Toll of Drug-Resistant Bacteria. *Nature* **2022**, d41586-022-00228–x. https://doi.org/10.1038/d41586-022-00228-x.

(50) Prestinaci, F.; Pezzotti, P.; Pantosti, A. Antimicrobial Resistance: A Global Multifaceted Phenomenon. *Pathogens and Global Health* **2015**, *109* (7), 309–318. https://doi.org/10.1179/2047773215Y.0000000030.

(51) *Challenges in Diagnosing Infection in ED*. Society for Academc Emergency Medicine. https://www.saem.org/education/industry-sponsored-education/challenges-in-diagnosing-infection-in-the-ed.

(52) Jia, Z.; Müller, M.; Le Gall, T.; Riool, M.; Müller, M.; Zaat, S. A. J.; Montier, T.; Schönherr, H. Multiplexed Detection and Differentiation of Bacterial Enzymes and Bacteria by Color-Encoded Sensor Hydrogels. *Bioactive Materials* **2021**, *6* (12), 4286–4300. https://doi.org/10.1016/j.bioactmat.2021.04.022.

(53) Sethi, S.; Datta, A.; Gupta, B. L.; Gupta, S. Optimization of Cellulase Production from Bacteria Isolated from Soil. *ISRN Biotechnology* **2013**, *2013*, 1–7. https://doi.org/10.5402/2013/985685.

(54) Song, Y.-S.; Seo, D.-J.; Jung, W.-J. Characterization and Antifungal Activity of Chitosanase Produced by Pedobacter Sp. PR-M6. *Microbial Pathogenesis* **2019**, *129*, 277–283. https://doi.org/10.1016/j.micpath.2019.02.026.

(55) Pilon, F. M.; Silva, C. da R.; Visôtto, L. E.; Barros, R. de A.; da Silva Júnior, N. R.; Campos, W. G.; de Almeida Oliveira, M. G. Purification and Characterization of Trypsin Produced by Gut Bacteria from *Anticarsia Gemmatalis*: PILON et Al. *Arch. Insect Biochem. Physiol.* **2017**, *96* (2), e21407. https://doi.org/10.1002/arch.21407.

(56) Fu, X. T.; Kim, S. M. Agarase: Review of Major Sources, Categories, Purification Method, Enzyme Characteristics and Applications. *Marine Drugs* **2010**, *8* (1), 200–218. https://doi.org/10.3390/md8010200.

(57) Chauhan, P. S.; Saxena, A. Bacterial Carrageenases: An Overview of Production and Biotechnological Applications. *3 Biotech* **2016**, *6* (2), 146. https://doi.org/10.1007/s13205-016-0461-3.

(58) Elyasi Far, B.; Ahmadi, Y.; Yari Khosroshahi, A.; Dilmaghani, A. Microbial Alpha-Amylase Production: Progress, Challenges and Perspectives. *Adv Pharm Bull* **2020**, *10* (3), 350–358. https://doi.org/10.34172/apb.2020.043.

Appendix

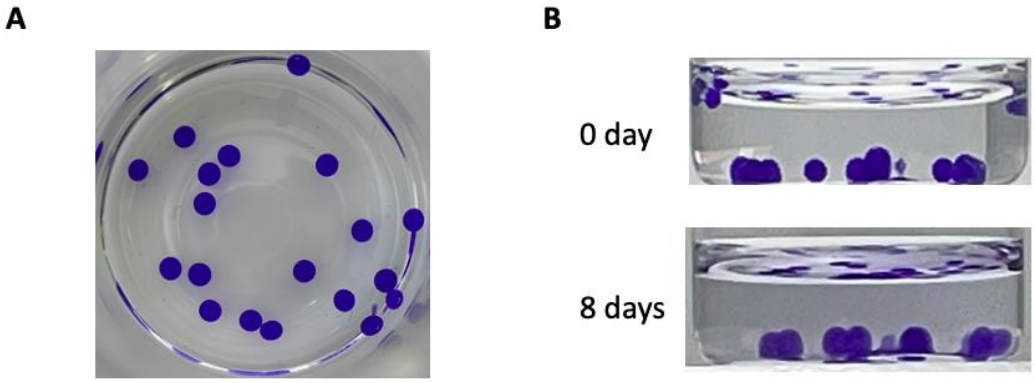

Figure A-1 Study of 0.6% calcium alginate/40% Dex 6k hydrogel beads. (A) Overall morphology. (B) Dye release study.

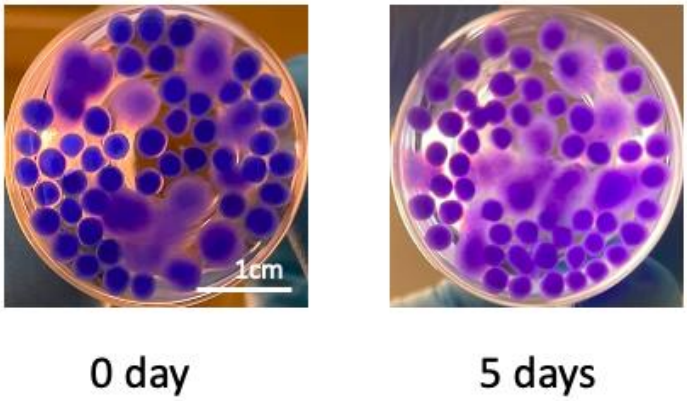

Figure A-2 Morphology, stability, and dye release studies of calcium 1.5% alginate/15% EOPO/0.375% carrageenan hydrogel beads.